UNIVERSIDADE FEDERAL DE SANTA CATARINA GRADUATION COURSE OF MATERIALS ENGINEERING

DIOGO BASTOS DE TOLEDO

X-RAY SCATTERING OF SPIN COATED POLYTHIOPHENE FILMS USING AN IN-HOUSE SOURCE

MAINZ

2009

UNIVERSIDADE FEDERAL DE SANTA CATARINA GRADUATION COURSE OF MATERIALS ENGINEERING

DIOGO BASTOS DE TOLEDO

X-RAY SCATTERING OF SPIN COATED POLYTHIOPHENE FILMS USING AN IN-HOUSE SOURCE

Thesis presented to the Graduation
Course of Materials Engineering from the
Universidade Federal Santa Catarina
"Engenheiro de Materiais"

Supervisor: Silke Rathgeber

MAINZ

2009

DIOGO BASTOS DE TOLEDO

X-RAY SCATTERING OF SPIN COATED POLYTHIOPHENE FILMS USING AN IN-HOUSE SOURCE

This work was assessed adequate to the attainment of the title “Engenheiro de Materiais” and approved by the Graduation Course of Materials Engineering from the Universidade Federal of Santa Catarina.

Assessment Committee

Dr. habil. Silke Rathgeber

Dr. Harald Hoppe

Dr. habil. Daniel Ayuk Mbi Egbe

DE TOLEDO, Diogo Bastos, 1982-

X-Ray Scattering of Spin Coated Polythiophenes Films Using an In-house Source/

Diogo Bastos de Toledo. – 2009

64f.: il. Color 30 cm.

Supervisor: Silke Rathgeber

Trabalho de Conclusão de Curso – Universidade Federal de Santa Catarina, Curso de Engenharia de Materiais, 2009.

1. X-ray scattering. 2. Polythiophene. 3. Spin coating. I. Rathgeber, Silke. II. Universidade Federal de Santa Catarina, Curso de Engenharia de Materiais. III. X-Ray Scattering of Spin Coated Polythiophene Films Using an In-House Source.

ACKNOWLEDGEMENTS

First of all, I would like to thank Professor Hans-Jürgen Butt for the opportunity to work in his group at the Max Planck-Institute for Polymer Research and for the infra-structure he offered me to develop this work.

Secondly, I thank my supervisor Dr. habil. Silke Rathgeber, for the trust in my work, technical and theoretical support, patience and care with which she supervised my diploma thesis.

A special thanks goes to Dr. Jochen Gutmann, for hosting me in his group at the Max Planck-Institute and the discussions, Michael Bach, for the x-ray scattering support, Dr. Mine Minesa, for the spin coating tips, Dr. Ingo Lieberwith for the transmission electron measurements and film removal help, Gunnar Kircher, Andreas Best, Tiago Rodrigues and all the members from Prof. Butt's group for the interesting talks and fun activities.

Thinking of my family, I would like to thank my mother Marilene Aparecida Bastos de Toledo and my father Tarcisio Silva Lourenço de Toledo, for the love and effort spent to show me the right way. Also my sisters Renata and Gabriela Bastos de Toledo for always be there throughout my development.

I would like to express my special thanks also to Natalie Kehle for the special moments, support, advice and English help.

Finally, I thank the Universidade Federal de Santa Catarina for the support and opportunities, and also the friends from the Materials Engineering course for the great moments throughout the course.

ABSTRACT

Polythiophenes is from a special class of polymers, conjugated polymers, in which π-orbitals are overlapped throughout the backbone due to the high number of carbon double bonds in the monomer of the backbone. This chemical characteristic makes for outstanding photoelectrical properties and creating high interest from the semiconductor industry. These polymers are also called synthetic metals and are of growing importance over the last decades due to its broad application and low production costs. Polythiophenes can be used mainly in thin film organic electronics, such as solar cells, thin film transistors and light emitting diodes. Nowadays, the main challenge that scientists and engineers face is to synthesize stable polymers that keep their properties over time and developing a production process that will optimize the device's properties with reproducibility.

Most of the application of polythiophenes uses the polymers in a film form, therefore the film production technique has a high importance on the development and improvement of the device efficiency. The most popular techniques are: drop casting, spin coating and inkjet printing. Several studies already showed that the electrical properties of the polythiophenes are influenced by the film preparation process. Therefore the importance to choose the right technique.

The motivation of this work is based on the evaluation of the influence of the film preparation using a spin coating process on the polythiophene's structure. This influence were measured performing wide angle x-ray scattering (WAXS) experiments using an in-house. Usually the x-rays measurements of thin films are performed in a synchrotron source, because this source has high energy, which enable measurements of sample that does not produce high scattering. Due to the sample preparation technique, this measurement could be made using a normal in-house source. Under these experiments, the films were produced by the spin coating technique using poly(3-hexyl-thiophene) and poly(3octyl-thiophene), both in regioregular conformation.

RESUMO

Politiofeno pertence a uma classe especial de polímeros, conhecida como polímeros conjugados, que possui π-orbitais sobrepostos devido ao grande número de dupla ligação entre átomos de carbono no monômero da cadeia polimérica. Essa característica resulta em propriedades photo-eletricas que não são comuns aos polímeros, criando dessa maneira, grande interesse da indústria em torno desses materiais. Também conhecidos com metais sintéticos, esses polímeros receberam grande atenção nas ultimas décadas por causa das diferentes possibilidades de aplicação bem como o seu baixo custo de produção. Politiofeno pode ser usado principalmente na produção de painéis solares, transistores e *light emitting diodes*. Atualmente os grandes desafios para os cientistas e engenheiros estão na síntese de polímeros estáveis que mantêm as propriedades elétricas em longo prazo e também em desenvolver um processo produtivo que aperfeiçoe as propriedades dos componentes com reprodutibilidade.

Grande parte dos componentes eletrônicos produzidos com politiofeno, utilizam o material na forma de filme, consequentemente o processo de produção desses filmes recebe grande importância no desenvolvimento e aperfeiçoamento da eficiência dos componentes. As técnicas mais populares de produção de filmes são: *drop casting, inkjet printing and spin coating*. Estudos já mostraram que as propriedades elétricas dos filmes de politiofeno esta diretamente ligada à técnica de produção dos filmes. Por isso a importância em escolher o método ideal.

A motivação desse trabalho esta em identificar a influencia da preparação dos filmes usando *spin coating*, na estrutura dos filmes de politiofeno. Essa influencia foi avaliada pelos experimentos de difração de raios-X em largos ângulos, em inglês wide angle x-ray scattering, usando uma fonte comum. Geralmente os experimentos feitos em filmes finos são realizados em aceleradores de partículas, pois essa fonte de raios-X possui alta energia, o que possibilita a avaliação de estruturas que não produz grande quantidade de difração. Por causa do método de preparação das amostras, foi possível realizar esses experimentos usando uma fonte comum.

LIST OF PICTURES

LIST OF TABLES

LIST OF SYMBOLS AND ABREVIATIONS

PT	polythiophene
UV	ultraviolet
P3AT	poly(3-alkyl-thiophene)
P3HT	poly(3-hexyl-thiophene)
P3OT	poly(3-octyl-thiophene)
HT	head to tail
HH	head to head
TT	tail to tail
Mw	molecular weight
HMDS	hexamethyldisilazane
OTS	octadecyltrichlorosilane
2D WAXS	two dimension wide angle x-rays scattering
SAXS	small angle x-ray scattering
q	scattering vector
XRD	x-ray powder diffraction
mm	millimeter
nm	nanometer
Hz	Hertz
µm	micrometer
cm	centimeter
HF	hydrofluoric acid
DSC	differential scanning calorimetry
TGA	thermal gravimetric analysis
GPC	gel permeation chromatography
GADDS	general detector diffraction system
d	inter chain distances
T	x-ray transmittance
s	thickness of the sample
I	transmitted intensity of the sample
I_0	transmitted intensity from the empty beam.
FWHM	full width at half maximum

TABLES OF CONTENTS

1. INTRODUCTION

1.1. POLYTHIOPHENE

Polythiophenes (PT) result from the polymerization of sulphur heterocycle monomers, called thiophenes. They become conducting when electrons are added or removed from the conjugated π-orbital via doping. The synthesis of polythiophenes plays an important role on the electrical properties; it can determine the magnitude of π-orbital overlap along the backbone and eliminate structural defects (the chemistry of conduct.). The polythiophenes chemically synthesized are moderately crystalline in a lamellar configuration and with a compact planar thiophenes structure with four monomers per unit cell [(17)], whereas Garnier et all[(18)], showed that electrochemically synthesized poly(3-methyl-thiophenes) can exhibit helical configurations with a close pack into a triangular array of these helices. Polythiophenes demonstrate interesting optical properties due to their conjugated backbone, as demonstrated by the fluorescence of a substituted polythiophene solution under UV irradiation [(19)].

The study of polythiophenes has intensified over the last three decades, due to the most notable property of this material, the electrical conductivity which results from the delocalization of electrons along the polymer backbone – hence the term “synthetic metals”. This property is intimately related to their molecular structures and intermolecular interactions. However, conductivity is not the only interesting property resulting from electron delocalization. The optical properties of this material responds to environmental stimuli; with dramatic color shifts in response to changes in solvent, temperature, applied potential, and binding to other molecules. Changes in both color and conductivity are induced by the same mechanism; twisting of the polymer backbone, disrupting conjugation, thereby making conjugated polymers attractive as sensors that can provide a range of optical and electronic responses [(19)].

1.1.1. Side Chains Impact

In order to improve the solubility and the processibility in common solvents, flexible side chains are introduced into the rigid backbone. This procedure also modifies the electronic

properties of the polymer, furthering the possibility for industrial applications. Typically, alkyl side chains are introduced into the polythiophenes backbone [1].

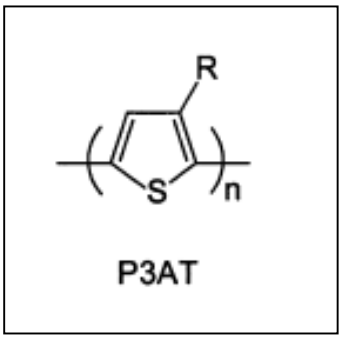

Figure 1.1: Poly(3-alkyl-tiophene) monomer [1]

The polymers chains from P3AT present a self organization, adopting a lamella type structure in a trans zigzag [15] model with two-dimensional conjugated sheets, formed by π–π inter-chain stacking and phase segregated layers of insulating alkyl side chains [7]. According to the values for the P3ATs d-spacing calculated by x-ray diffraction, Chabinyc [13] suggested an end-to-end structure regarding the side chains of the conjugated backbone (Figure 1.2), in which the end of the side chains faces the end of the side chain from the neighbor backbone.

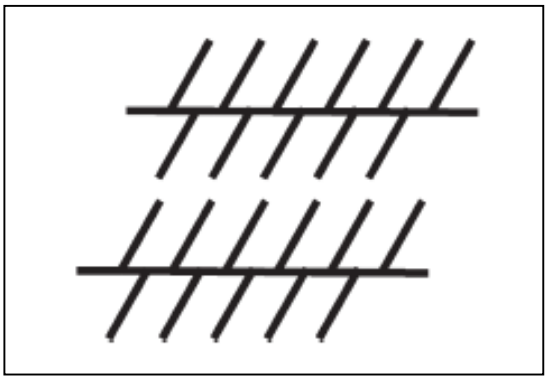

Figure 1.2: end to end structure [13]

The crystalline structure of PATs consists of planar configuration in a rigid rod conformation, in which the backbone comprises a nearly linear arrangement of aromatic repeated units separated by the side chains. The combination of the conjugated (backbones) and non-conjugated (side chains) regions leads to a high ordered structure due to the driving force of separation of these two regions [13]. The polymer chains are stacked on top of each other; the stacking distance is denoted as the b-axis and the repetition distance along the main chain is denoted as the c-axis. The bc layers are separated by the alkyl side chains,

corresponding to the a-axis [4]. The charge mobility along this axis should be lower due to the relatively poor electronic coupling between the σ-system of the side chains and the π-systems of the backbone.

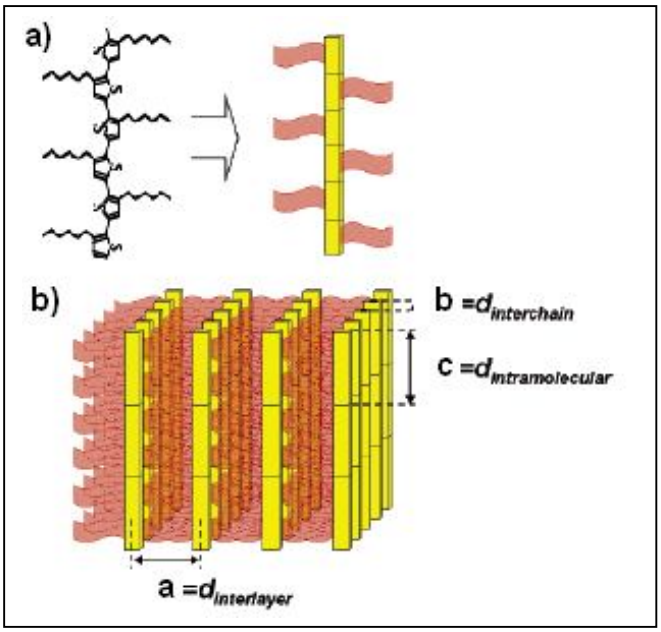

Figure 1.3: Poly(3-alkyl-thiophene) unit cell

1.1.2. Regioregularity Influence

The optic-electronic properties are not only modified by the side chains, but also by the regioregularity, the molecular weight and the film production technique. Due to the asymmetry of the 3-substituted thiophenes, three possible couplings are possible when two monomers are linked; the head to tail (HT), head to head (HH) and tail to tail (TT) (Figure 1.4). From these three diads, four triads can be combined. A regioregular P3AT has a high ordered sequence of monomer on the backbone, whereas a regiorandom has a random order of monomers in the backbone. This ordering produces consistent differences on the optic-electrical properties of the polymers [14]. Films of regioregular P3AT show a semi-crystalline and bronze-colored film with a metallic aspect, on the other hand, the corresponding regiorandom polymers produced amorphous and orange-colored films. A high regioregularity of the P3AT leads to a higher mobility charge, due to a higher ordering, higher crystallinity and overlap of the π orbital than the samples with a lower regioregularity.

1.1.3. Molecular Weight (Mw) Influence

The charge mobility of the P3AT is also influenced by its molecular weight, whereby increasing this parameter also increases the mobility. A model that explains well this characteristic was proposed by Neher [6]. He suggested that the samples from P3AT with a low molecular weight consists mainly of disordered domains with crystallites of high ordered chains separated by grain boundaries, whereas the samples with a long chain fraction or at least partially ordered domains present the chains organized in crystalline. In this case, the charges can move parallel to the layer plane through percolation pathways, instead of being trapped by grain boundaries.

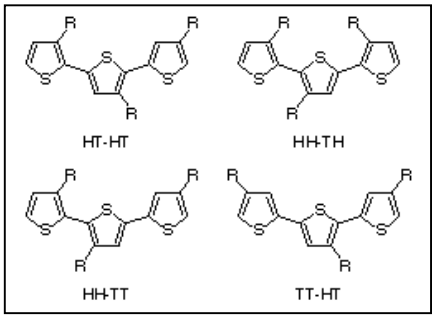

Figure 1.4: The four possible triads in the PT backbone [19]

1.1.4. Rotational Speed Influence

Films produced from conjugated polymers have a polycrystalline structure, which are composed of a mixture of ordered and disordered regions, whereby both regions will impact the electrical property [13]. The charge transport in ordered domains is anisotropic and the carriers must travel through many domains during the operation. Thus, the orientation relative to each other and to the substrate has to be taken into consideration to understand the charge mobility.

The final microstructure of the films is greatly influenced by its production process. Spin coating, for example, is a non-equilibrium technique that is driven by centrifugal forces on the molecules during the spinning process and by the evaporation rate of the solvent. Comparatively, the drop casting technique is driven only by the solvent evaporation rate. The films produced by drop casting show a microstructure closer to the equilibrium, with

distances between the polymer planes smaller and the charge mobility higher than the films produced by the spin coating technique [13].

In particular, the rotational speed for spin coating plays an important role on the microstructure of the film. The higher the rotational speed, the higher the centrifugal forces and the evaporation rate, thereby decreasing the time for the organization of the polymer chains inside the film. Films produced with high rotational speed of around 33,33 Hz exhibit a higher number of face-on conformation of the lamellas with the side chains of the polymer lying in the substrate plane, Figure 1.6 [9,11]. On the other hand, films spun with low rotational speeds (4,16 Hz) exhibit an edge-on conformation with the side chains perpendicular to the substrate plane, Figure 1.5 [9,11].

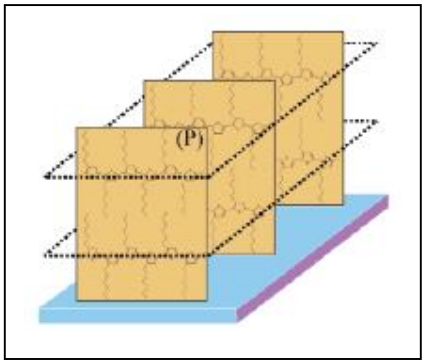

Figure 1.5: edge-on conformation [9]

1.1.5. Cast Solvent Influence

The solvent has a strong influence on the morphology of the films due to the interactions with the aggregate polymer chains during the drying process. The solvent is expected also to have an influence on the crystallinity of the film and therefore to its electrical properties. A slow solvent evaporation speed facilitates the growth of a highly crystalline film, the inter-chain interactions becomes stronger and thus improve the electro-conductivities considerably [12].

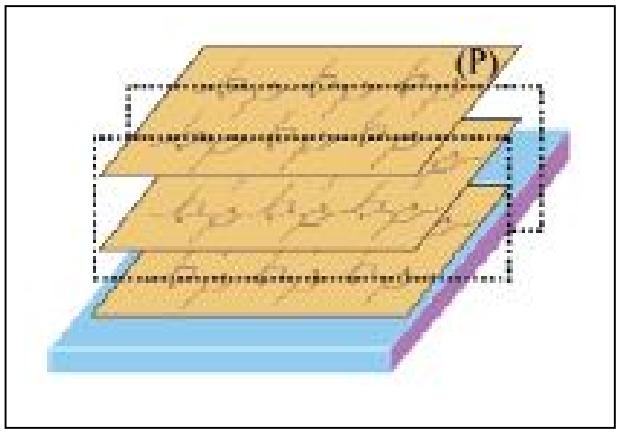

Figure 1.6: face-on conformation [9]

1.1.6. Surface Influence

Studies performed on films spun on a hydrophobic substrate showed that the crystallization is also influenced by the substrate surface, resulting in a significant improvement of the charge mobility. Typically, the hydrophobization is made with a silane component. This treatment changes the morphology of the crystallites close to the surface with the substrate, which is highly related to the electron mobility of the PAT films. Scavia et al [20], showed that even the length of the silane, has an influence on the electronic properties of the P3HT films. Silane components with substituents having a short length like hexamethyldisilazane (HMDS) organizes the crystallites in terms of filaments, whereas using a long chain component, like octadecyltrichlorosilane (OTS) a different globular morphology occurs where the π-π stacking are organized in a shorter and thinner needle-like morphology.

This last morphology has higher efficiency on the charge mobility because it has "exposed" π orbitals all along its long axis, which increase the possibility of a π orbital overlap with the adjacent needles, therefore the charge mobility occurs easily than in filament morphology. In this configuration only the chains at the extremes of the filament or at its bended part have π orbitals exposed, thus it has a high number of π orbitals overlapping within the filament, but a low number of this overlap with the adjacent filaments. In case of a bare substrate, the crystallites have morphology of filaments similar to the surface treated with DMDS, but it does not show the bending of the filament like this last one shows. Therefore the π orbital overlap between adjacent filaments is decreased.

1.1.7 Thermal Treatment Influence

The packing structure has a strong effect on the influence on the electrical transport of semiconductor polymers, therefore a thermal treatment would be advantageous to re-organize the molecules in the film. The heating process anneals the films and remove packing defects. The re-organizing process is believed to be driven by the disordering of the ordered side chains upon heating, which increases the lamellar d-spacing. This process allows the polymer molecules to become more mobile and slip within the neighbor lamella. In this case, the side chains act as “bound solvent” [(13)].

1.2 SPIN COATING

The spin coating is a popular procedure, being used for several decades to apply uniform, thin films to flat substrates. This common process involves depositing the solution with the polymer base of the film dissolved, onto the centre of the substrate and then spinning the substrate at high speed. The solution is spread by centripetal forces caused by the rotational speed of the substrate, until the fluid spins off the edges of the substrate and until the desired thickness of the film is achieved. Final film thickness and other properties will depend on the nature of the resin, such as viscosity, drying rate, percent solids and surface tension.

The parameters chosen for the spin process, like rotational speed, acceleration and fume exhaust contribute to how the properties of coated films are characterized. The applied solvent is usually volatile and simultaneously evaporates. One of the most important factors in spin coating is the repeatability; variations in the parameters of the procedure can result in drastic variations in the coated film. The spin process is described in the Figure 1.7.

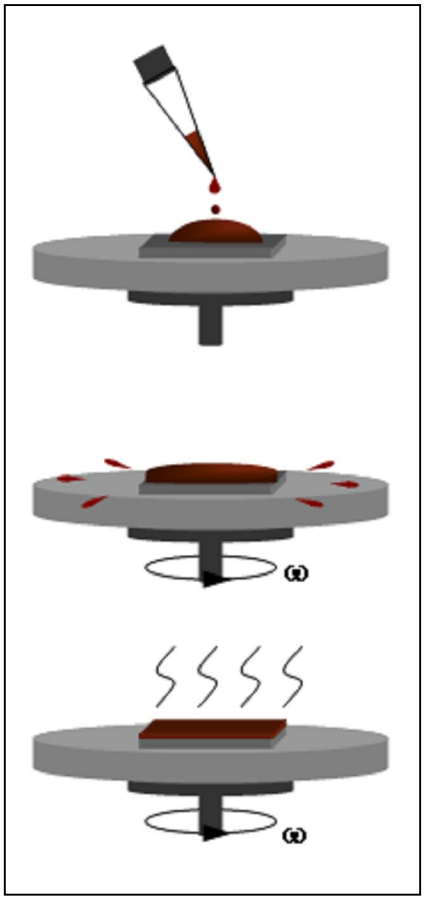

Figure 1.7: Sketch from spin coating process [24]

The dispense step in which the solution is deposited onto the substrate surface, can be divided in Static or Dynamic dispense. The static version is simply depositing the solution on or near the centre of the substrate; the amount of the solution to be disposed depends on the viscosity of the solution and the size of the substrate. For higher viscosity solutions or larger substrates, a larger amount is required to ensure full coverage of the substrate during the high speed spin step. Dynamic dispense is the process of dispensing while the substrate is turning at low speed. This serves to spread the solution over the substrate while resulting in less solution waste since it is usually not necessary to deposit as much to wet the entire surface of the substrate. This is a particularly advantageous method when the solution or substrate itself has poor wetting abilities and can eliminate voids that may otherwise form.

After the dispense step, it is common to accelerate to a relatively high speed to thin the solution to near its final desired thickness. It can also affect the coated film properties. Since the resin begins to dry during the first part of the spin cycle, it is important to accurately control acceleration. In some processes, 50% of the solvents in the resin will be lost to

evaporation in the first few seconds of the process. Acceleration also plays a large role in the coat properties of patterned substrates. In many cases the substrate will retain topographical features from previous processes, it is therefore important to uniformly coat the resin and through these features. While the spin process in general provides a radial (outward) force to the resin, it is the acceleration that provides a twisting force to the resin. This twisting aids in the dispersal of the resin around topographic areas that might otherwise shadow portions of the substrate from the solution.

Spin speed is one of the most important factors in spin coating. The speed of the substrate affects the degree of radial (centrifugal) force applied to the liquid resin as well as the velocity and characteristic turbulence of the air immediately above it. In particular, the high speed spin step generally defines the final film thickness. Relatively minor variations of ±50 rpm at this stage can cause a resulting thickness change of 10%. Film thickness is largely a balance between the force applied to shear the solution towards the edge of the substrate and the drying rate that affects the viscosity of the resin. As the resin dries, the viscosity increases until the radial force of the spin process can no longer appreciably move the resin over the surface. At this point, the film thickness will not decrease significantly with increased spin time.

The slower rate of drying offers the advantage of increased film thickness uniformity across the substrates. The fluid dries out as it moves toward the edge of the substrate during the spin process. This can lead to radial thickness non-uniformities since the fluid viscosity changes with distance from the centre of the substrate. By slowing the rate of drying, it is possible for the viscosity to remain more constant across the substrate.

The drying rate of the solution during the spin process is defined by the nature of the solution itself; volatility of the solvent systems used as well as by the air surrounding the substrate during the spin process. The resin will dry depending on the ambient conditions around it, such as air temperature and humidity. These influences are well known to play a large role in determining coated film properties. It is also important that the airflow and associated turbulence above the substrate itself be minimized or at least held constant, during the spin process.

Variations of only a few percent relative humidity can result in large changes in film thickness. By spinning in a closed bowl, the vapors of the solvents in the resin itself are retained in the bowl environment and tend to minimize the affects of minor humidity variations. At the end of the spin process, when the lid is lifted to remove the substrate, full exhaust is kept to contain and remove solvent vapors. Another advantage to this “closed

bowl" design is the reduced susceptibility to variations in air flow around the spinning substrate. Various factors affect the local properties of this air flow. Turbulence and eddy currents are common results of this high degree of air flow. Minor changes in the nature of the environment can create drastic alteration in the downward flow of air [22]. By closing the bowl with a smooth lid surface, variations and turbulence caused by the presence of operators and other equipment are eliminated from the spin process.

The residual film thickness depends not only on the spinning velocity, but also on the solution concentration and on the molar mass M of the solution. These parameters will increase the viscosity of the solution, therefore its wetting ability will be higher as well as the final film thickness.

Spin coating is widely used in micro-fabrication of electronic components, where it can be used to create thin films with thicknesses below 10 nm. It is used intensively in photolithography, to deposit polymer layers about 1 micrometer thick.

1.3. WIDE ANGLE X-RAY SCATTERING

Wide Angle X-ray Scattering (WAXS) is an x-ray diffraction technique that is often used to determine the crystalline structure of polymers. This technique specifically refers to the analysis of Bragg Peaks scattered at wide angles, which (by Bragg's law) implies that they are caused by sub-nanometer sized structures [21]. WAXS is a similar technique as Small-Angle X-ray Scattering (SAXS), having only the distance from sample to the detector shorter and thus diffraction maxima at larger angles are observed, usually larger than 5°. SAXS is used to measure relatively long range inter planar distances, such as the domain size of the ordered regions. WAXS on the other hand, is used to probe smaller distances, usually in short range order and it is more common then SAXS for semiconductor polymer measurements.

According to this method, the sample is scanned in a wide angle X-ray goniometer, and the scattering intensity is plotted as a function of the 2θ angle or at the magnitude of the scattering vector (q). X-ray diffraction is a non-destructive method of characterization of solid materials; when x-rays are directed into solids, they will scatter in predictable patterns based upon the internal structure of the solid. A crystalline solid consists of regularly spaced atoms (electrons) that can be described by imaginary planes. The distance between these planes is called the d-spacing. The intensity of the d-space pattern is directly proportional to the number of electrons (atoms) that are found in the imaginary planes. Every crystalline solid

will have a unique pattern of d-spacing (known as the powder pattern), which is a finger print for that solid. In fact, solids with the same chemical composition but different phases can be identified by their pattern of d-spacing.

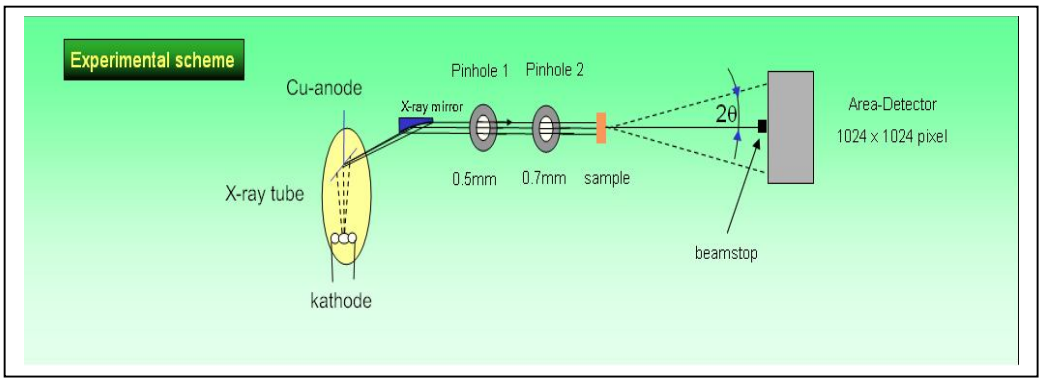

Figure 1.8: Sketch from the 2D WAXS equipment at Max-Planck-Institute for Polymer Research – Mainz

In a WAXS instrument, a monochromatic beam of X-rays is brought to a sample from which some of the X-rays scatter, while most simply go through the sample without interacting with it. The scattered X-rays form a scattering pattern that is then identified by a detector; typically a two-dimensional flat X-ray detector situated behind the sample, perpendicular to the direction of the primary beam that initially hit the sample. The scattering pattern contains the information on the structure of the sample.

The x-ray experiments can be performed using different configurations. In the case of this work, 2 Dimension Wide Angle X-rays Scattering (2D WAXS) and X-ray Powder Diffraction (XRD) technique were used. In the first technique with the sample surface is placed perpendicular to the x-ray incident beam, which results in a scattering vector parallel to the surface. In this configuration the structures probed will be perpendicular to the sample surface. The XRD technique is performed varying the angle between the incident x-ray beam and the sample surface. The resulting scattering vector of this technique is perpendicular to the surface sample, which probe structures parallel to the sample surface. The diffraction pattern generated allows the characterization of the chemical composition or phase composition of the film, the texture of the film (preferred alignment of crystallites), the crystallite size and presence of film stress.

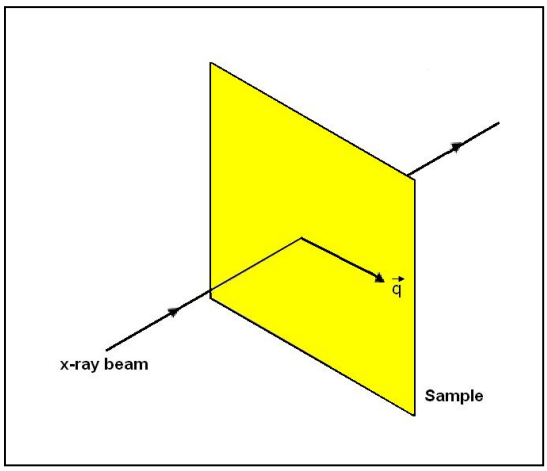

Figure 1.9: Sketch from 2D WAXS technique

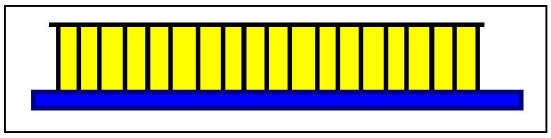

Figure 1.10: Sample probed by the 2D WAXS technique

In the case of thin film scattering for conventional x-rays sources, longer exposure times in the X-ray beam are required due to the relatively weak scattering strength of carbon, small number of scattering planes as well as the disorder in these films. Therefore, only the strongest peaks are observed.

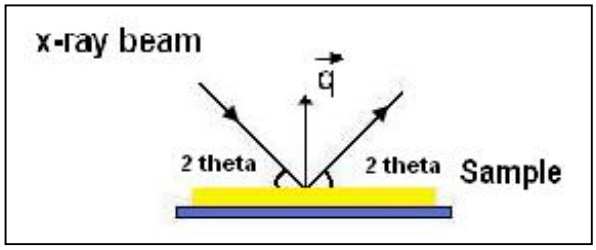

Figure 1.11: Sketch from the XRD technique

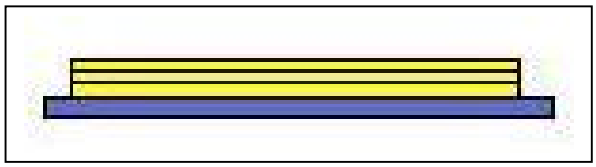

Figure 1.12: Samples probed by the XRD technique

The major problem that must be overcome in WAXS instrumentation is the separation of the weak scattered intensity from the strong main beam. The smaller the desired angle, the more difficult this becomes. The non-scattered beam that merely travels through the sample must be blocked, without blocking the closely adjacent scattered radiation. Most available x-ray sources produce divergent beams and this compounds the problem. In theory, the problem could be overcome by focusing the beam, but this is not easy when dealing with x-rays and was previously not done except on synchrotron where large bent mirrors can be used.

The 2D WAXS at the Max-Plank-Institute in Mainz uses an x-ray beam with a pinhole collimation and a two-dimensional detector (Siemens Serial A102647) with 1,024 pixels. A double graphite monochromator for the CuKα radiation (λ= 0.154 nm) was used. The beam diameter is about 0.5 mm and the sample-to-detector distance was 73mm. The patterns were recorded with vertical orientation of the filament axis and with the beam perpendicular to the sample.

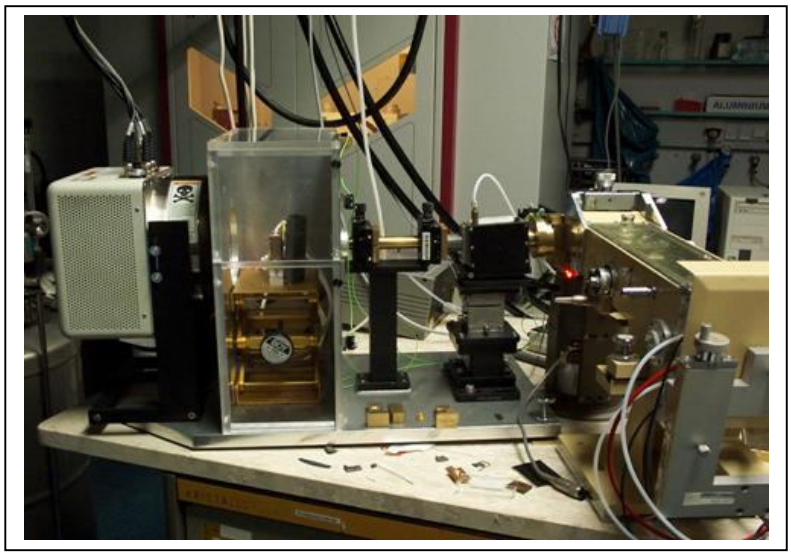

Figure 1.13: Picture from the 2D WAXS equipment from Max-Planck-Institut for Polymer research

2. EXPERIMENTAL METHODS

2.1. SAMPLE PREPARATION

The sample preparations played a vital role in this project as it influences the results of the measurements. Every step requires careful consideration for optimal results. The sample preparation procedure involved substrate cleaning, solution preparation, spin coating and the removal of the films from the substrate. Four samples of polythiophene were used, two poly(3-hexyl-thiophene), one with regioregular and other with rediorandom conformation. Two samples of poly(3-octyl-thiophene) were also used, both regioregular and rediorandom conformation. The samples were supplied by Sigma Aldrich (Germany).

2.1.1. Substrate Cleaning

Glass substrates, supplied by Menzel GmbH (Brauschweig, Germany), were used for the sample preparation. The dimensions were 2.5 x 2.5 centimeters. Before the film casting, the glass substrates were cleaned with an ammonium solution. This ensures that the surface is clean and free of grease and particles, thereby improving the quality of the film. The treatment consists of immersing the substrates in an ammonium solution of 28%, hydrogen peroxide solution of 35% and miliQ water at a proportion of 1:1:5, respectively, for thirty minutes at a temperature of 60 °C. Subsequently, they were washed with miliQ water and dried with compressed nitrogen. The surface presented high hydrophilicity (the contact angle was too small to be measured with water) and a high reproducibility.

2.1.2. Hydrophobic Treatment

As described in section 1.1.6, the surface of the substrate has a strong influence on the crystallization and on the structure of the films. In order to evaluate this influence, films of poly(3-hexyl-thiophene) regioregular were produced using a hydrophobic substrate. The hydrophobic treatment consists of a vapor deposition of hexamethyldisilazane (HMDS), which was made after the cleaning process with an ammonium solution. The substrates were placed into a glass container with 4 drops of (HMDS) then closing this container to ensure that the silane would not escape, thereby creating an atmosphere with this composite. Finally,

the glass container with the substrates was put into an oven for one hour at 80 ºC, thus producing the vapor deposition of HMDS. After this procedure, the substrates showed a contact angle measured with water at around 74º.

2.1.3. Solution Preparation

The solutions were prepared using two different solvents; chloroform and chlorobenzene, both with a concentration of 10mg/ml. The main reason of using different solvents is due to their varying boiling points, which lead to different evaporation rates and different structural organization. The lower evaporation rate increases the time available for the chain alignment and facilitates the growth of a highly crystalline film with stronger inter-chain interactions [9, 11, 12]. This property improves the charge mobility in the film later. Those structural differences will be measured with wide angle x-rays scattering experiments. All the solutions were immersed in an ultrasonicated bath for one hour and then filtered before spinning with hydrophobic PTFE filter (0.20 µm pores size) to remove possible aggregates and dust.

2.1.4 Film Preparation

The procedure used to prepare the film was the spin coating technique because it is a simple and flexible technique with high reproducibility. By changing the parameters of the technique, the microstructure of the film can also be changed, as explained in section 1.1.4. One of the aims of this work was to evaluate the influence of the spin speed on the polymer structure of the films, which were produced using spin speed of 4,16 and 33,33 Hz.

This film preparation was not only focused on the rotational speed influence, but also the influence from the evaporation rate of the solvent on the structure of the films. Two different solvents were compared in this work. The first one was chloroform, which has a high vapor pressure (26 KPa at 25 ºC). The second one was chlorobenzene, which has a low vapor pressure (1.6 KPa at 25 ºC). Since chloroform has a faster evaporation rate, less spinning time was required (60 seconds for 4,16 Hz and 15 seconds for 33,33 Hz) compared to chlorobenzene, which has a lower evaporation rate and needed 300 seconds for 4,16 Hz and 60 seconds for 33,33 Hz to dry the solvent and produce the film. Even with different solvents properties, films spun from chloroform and chlorobenzene showed comparable thickness, around 300 nm for the films spun at 4,16 Hz and around 150 nm for the films spun at 33,33

Hz. The thickness of the films were measured by a confocal microscope from the Max Planck Institute for Polymer Research, supplied by Nanofocus AG (Oberhausen Germany) and using the µsurf software, supplied by the same company.

As mentioned earlier, the spin speed has a significant influence on the structure of the film, especially concerning its thickness. The spinning of the solutions with a low speed (4,16 Hz) presented thicker corners than on the rest of the substrate. The centrifugal forces were not strong enough to expel all the solution out of the substrate and after the spinning some solution accumulates at the corners. However, these lower forces also produce thicker films than the films spun with high speeds. To produce a homogeneous film, especially using lower speeds, the solution had to be spread all over the substrate before the spinning because the centrifugal forces were not strong enough to spread the solution and form a homogeneous film.

Tests using 1,2,4-trichlorobenzene were also performed, but the spinning of the trichlorobenzene solutions was not successfully done. This solvent has a vapor pressure of 38.6 KPa at 25ºC, which produces a low evaporation rate and requires a longer spinning time to dry the film. However, when such a solution is spun for a long time without reasonable evaporation, the solution will automatically accumulate at the corners of the substrate, due to the centrifugal forces from the rotational speed. Thus, at the end of the process only a thin layer of polymer and drops of the solution remain at the corners. The polymer film from this process was too thin to be measured by the confocal microscopy, therefore its application became inconvenient for the x-ray experiments proposed in this work. The photovoltaic industry usually applies a different technique to spinning of the trichlorobenzene solution, in which the solution is spun only for a few seconds to form a wet film and later this film is dried in a hot plate surface. Due to time constraints under the project, this technique could not be applied.

2.1.5. Film Removal

The removal of the films from the substrate was a key step for the sample preparation because it allowed the measurement of the samples by a transmission x-ray configuration using an in-house source. Scattering of films with thickness lower than 5µm is too low and requires a longer time to obtain reasonable statistics from the diffraction plans, which makes the experiments impractical. Another problem was the scattering from the glass substrate, which comparing to the scattering from the film would be much higher, because of the higher

thickness of a glass substrate (0.5 mm). The solution to these problems was to remove the films from the glass substrates and stack them on top of each other to produce a thicker film, which would produce consistent statistics in a reasonable measuring time (two hours).

The procedure consists of carefully immersing the glass substrates, with the dried films on the top, in a glass container full of water, at an angle of around 45° with the plane of the water surface. Due to the strong surface energy of the water and the low bounding forces between the film and the substrate, the film began to peel off the substrate and float on the water. This process does not provide any mechanical stress on the film, thus the orientation of the polymer chains remain the same as when it was on the substrate. The floated films were removed from the water using a Teflon square piece. This material made the removal of the sample from the “fishing” holder easier. After placing the floating films on the Teflon piece and removing them from the water, the films had to be dried using a heating gun with low temperature and low air flow. This step was necessary to ensure that the films on the Teflon piece would not float when it was re-immersed again in the water to place the next floating film.

The films had to be carefully piled on top of each other. The low thickness of the films reflected in low mechanical properties, which made the process more complicated because the films could be easily be damaged. The glass substrate used for the spinning had a square dimension of 2.5 x 2.5 cm^2. The x-ray source from the equipment had a beam diameter of a half millimeter. Thus the area exposed to the beam was much smaller than the area from the glass substrate. Such a big area was not necessary and it would make film removal more difficult. Therefore the 2.5 square centimeter films were divided into four pieces and piled on top of each other, making a thicker film with a square shape and size of about 1 x $1cm^2$.

As explained above, the outer parts of the spin coated films with 4,16 Hz exhibit an inhomogeneous thickness due to material accumulation at the corners of the substrate. Hence the edges of the films were removed and only the inner and more homogeneous part of the film was used. In this process the orientation of the molecules in the film was also taken into consideration. It is believed that the inner part of the film could show a lower orientation than its outer part, due to the increase of the centrifugal forces from the rotational speed with the distance from the centre of the sample. Therefore the films were piled up respecting this orientation and all of them were placed on top of each other in the same position. The samples prepared from the films spun with 4,16 Hz was a total of 28 films stacked on top of each other, whereas the sample from the films spun with 33,33 Hz films needed a total of 45 films

stacked to produce a similar thickness since they had a lower thickness than the films from the lower rotational speed.

Stacking the films showed some inconveniences; it was not possible to place the films exactly at the same place as the previous one, especially the films from P3HT that showed a brittle behavior and a tendency to rip apart when peeling off from the substrate. These difficulties brought some variations in the final thickness of the sample. Even stacking the same number of films showed a difference in the final thickness of sample. Every sample had its thickness measured using a precision clock; these measurements also showed variation of the thickness through the whole sample.

An optimal measuring thickness had to be stipulated at a minimum of 20 µm to produce consistent scattering intensity within a reasonable time. The final thickness of the sample was much lower, between 5 and 10 µm. The production of a sample with such thickness would be inconvenient due to the work and time consumed. Thus the samples had to be folded in two for the 4,16 Hz films and in four for the 33,33 Hz films to ensure minimum scattering intensity.

The polythiophene films have a hydrophobic character resulting in a higher interaction with the hydrophobic surface than with the hydrophilic one; therefore they could not be peeled off using only water. Thus the films spun on the glass substrate treated with HMDS had an additional step before peeling off the films with water. Floating of the film was realized by immersing the substrates with the films in a solution of water and 2.5% of hydrofluoric acid (HF) for 2 minutes before immersing them in the water. This acid is highly corrosive and toxic, but it was the only option since it is the only acid able to corrode glass and without damaging the polythiophenes films. After this additional step, the rest of the procedure was performed as the others.

2.2. X-RAYS EXPERIMENTS

Before the x-ray experiment, additional measurements were preformed to have a better understanding of the physical and chemical properties from the samples. Differential scanning calorimetry (DSC) experiments were performed to identify the temperature at which the phase transition occurs; this helped to set the appropriate temperature during the x-ray measurements in the temperature cycle as to measure the phase transition. In order to identify the decomposition temperature of the samples and also to determine the highest temperature

to be used in the x-ray equipment without damaging the structure of the sample, measurements with thermal gravimetric analysis (TGA) were made. Experiments with gel permeation chromatography (GPC) were also performed to have an estimation of the molecular weight (Mw) and the polydispersity of the samples. Standards of polystyrene and THF as a solvent was used. The molecular weight (Mw) could not exactly be calculated, since polythiophene standards are not available for this technique.

Table 2.1: Physical and chemical properties of the sample

	P3HT regioregular	*P3HT regiorandom*	*P3HT regioregular*	*P3HT regiorandom*
Transition Temperature	170- 230 ºC	-	140-180 ºC	-
Decomposition Temperature	~350 ºC	~310 ºC	~300 ºC	~300 ºC
Regioregularity	>98.5% HT	-	>98.5% HT	-
Molucular Weight (Mw)	~34,000	~85,000	~64,000	~59,000

The x-ray measurements were performed with an in-house wide angle x-ray scattering (WAXS) equipment because the samples presented diffraction within the angle range of this technique. The specifications of the WAXS equipment from the Max-Planck-Institute were already described in Section 1.3. After the measurements, the data had to be properly treated to ensure a precise result. The software General Detector Diffraction System (GADDS) version 4.0 (Bruker AXS, Wisconsin USA) was used to make the background subtraction to minimize the influence of air on the diffraction pattern.

The same software was also used to calibrate the beam center and the distance of the sample from the detector, using silver behenate as a standard. Both the silver behenate and the background were measured for every day that measurements were performed to ensure the precision of the measurements. The recorded scattered intensity distributions were integrated over the azimuthal angle by the same software and saved as a txt format. After this step, the data was transferred to Origin (8.0) to plot the graphs of the x-ray's diffraction, expressed by values of the scattering vector q and intensity of the diffraction. The scattering was calculated using equation 1, where θ is the scattering angle and λ is the x-ray wavelength.

$$q = \left(\frac{4\pi}{\lambda}\right)\sin\theta \qquad (1)$$

According to Bragg's Law, the inter-planar spacing (d_{hkl}) between parallel crystallographic planes (hkl) could also be calculated. Equation 2 was used to calculate the d-spacing of the crystallographic planes corresponding to the peak position q* of the Bragg-peak [23].

$$d = \frac{2\pi}{q^*} \tag{2}$$

2.2.1. Background Correction

The background correction played an important role on the evaluation of the data. Making an excessive or an insufficient subtraction of the background, the intensity of the peaks could then be easily changed. Thus, information from the sample could be hidden or over evaluated. This problem increases with the decrease of the sample thickness because less x-ray would be scattered by low quantity of material. A good illustration of background subtraction was made for the P3HT film spun with 4.16 Hz from chlorobenzene, Figures 2.1 and 2.2. Increasing the factor of subtraction results in a decrease in the height of the peaks, especially the ones at low q values where the scattering of the background is higher. Particularly for this sample, which has high peak at high q range, an incorrect interpretation could be made. The subtraction was made comparing the shape of the first order peak coming from the distances between the backbones localized at low q range. The subtraction factor was chose when the shape of the first peak was symmetric and the second order peak could be seen.

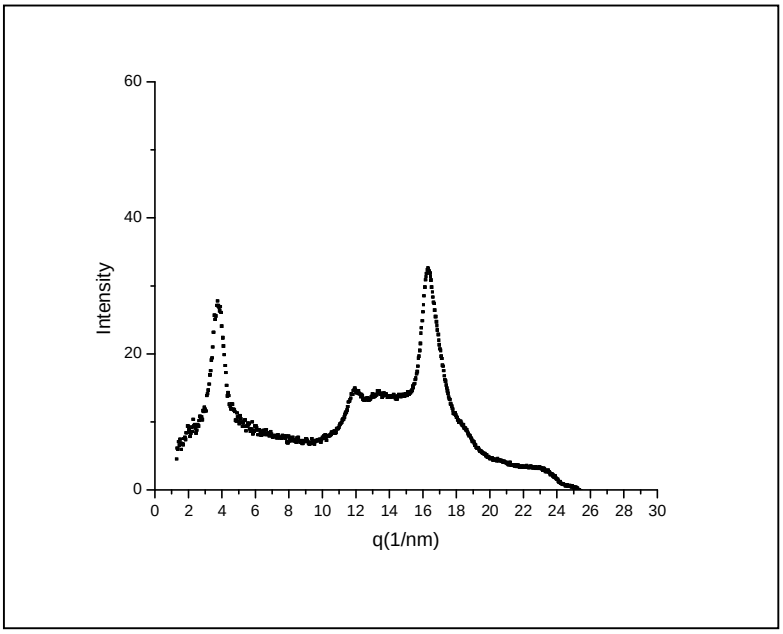

Figure 2.1: Diffraction pattern P3HT film after 0.95 background subtraction

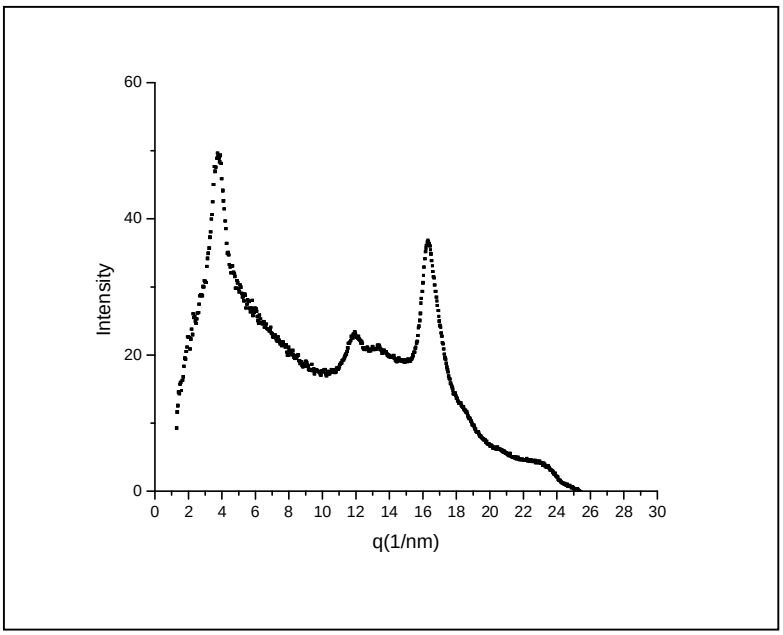

Figure 2.2: Diffraction pattern P3HT film after 0.85 background subtraction

3.2.2. Thickness Calibration

As explained earlier, the thickness of the sample had a significant effect on the scattering intensity. Since the samples showed variation in thickness, it was important to

normalize the intensity of the peaks. The x-ray transmission T can be expressed in terms of the sample thickness s:

$$T = \exp(-k*s) \tag{3}$$

Here k is the material constant. The transmission can also be expressed by the transmitted intensity of the sample (I), and by the transmitted intensity from the empty beam (I_0).

$$T = \frac{I}{I_0} \tag{4}$$

The transmitted intensities were obtained from the GADDS software, which calculated the number of counts from the beam spot of the 2D pattern from the samples and empty beam. Instead of calculating the real thickness of the sample, the two equations were joined to stipulate a thickness factor and normalize the intensity of the peaks, using the following equation:

$$\frac{\ln T_1}{\ln T_2} = \frac{s_1}{s_2} \tag{5}$$

To calculate the thickness factor, the samples which showed the lower thickness were chosen as a standard. Since two different polythiophenes were measured, two different standards were used.

2.2.3. Error Calculation

The errors calculation from the measurements played an important role on the data evaluation because it allowed the interpretation of the results and the conclusion of the measurements. This error was calculated using the measurements from the Ag-behenate used to calibrate the peak position (q*) of the diffraction patterns. The Ag-behenate has a well known structure with high crystallinity showing narrow diffraction peaks in a well defined q* position. Standard deviation of the peak position from the Ag-behenate measurements was calculated using the Origin software. Knowing the error from the Ag-behenate measurements,

the error of the measurements from the samples could also be calculated applying the error propagation formula. In the case of the calculation of the d-spacing error, the formula was as follows.

$$\frac{q*}{\Delta q*} = \frac{d}{\Delta d} \tag{6}$$

Where q is the q position of the diffraction peak from the sample, $\Delta q*$ is the standard deviation of the Ag-behenate q*, d is the d-spacing calculated from the peak position and Δd is the error from the d-spacing.

2.2.4. Full Width at Half Maximum

During the evaluation of the data from the x-ray measurements, the full width at half maximum (FWHM), Figure 2.3, was calculated from the first order peak coming from the distances between the backbones. For a precise calculation, the systematic error of the equipment was taken into consideration. The same was done for the error calculation; the error of the FWHM was also calculated using the measurements of the Ag-behenate. The FWHM of the peaks from the samples and also from the Ag-behenate were calculated by the fitting function with the Origin software. The standard deviation from the FWHM of the Ag-behenate measurements were also calculated using the same software. A convolution was used to calculate the real width of the diffraction patterns of the samples.

$$Sconv(q) = \int_{-\infty}^{\infty} \mathrm{Re}\, sol(q') * S(q - q') dq' \tag{7}$$

Where $Sconv(q)$ is measured peak shape broadened by the experimental resolution. $\mathrm{Re}\, sol(q')$ is the peak shape of the Ag-behenate which is assumed, due to the long range order in the material, to be solely broadened by the experimental resolution. $S(q - q')$ denotes the real peak shape of the sample. Assuming for all peaks a Gaussian shape the integral in Equation (7) can be easily solved and one obtains for the FWHM:

$$w_c^2 = w_r^2 + w_s^2 \tag{8}$$

Where w_c is the width of the measured sample by the equipment, w_r is the average values from the Ag-behenate measurements and w_s is the real width of the diffraction peaks from the samples.

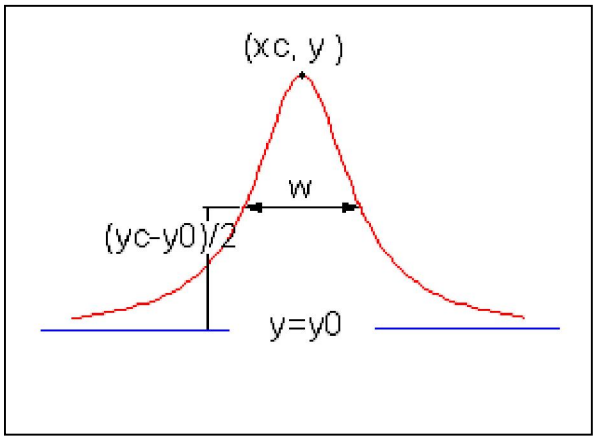

Figure 2.3: Full Width at Half Maximum

2.2.5. Domain Size Calculation

The domain sizes were calculated using the values of the FWHM from the first order peak coming from the distances between the backbones, where ξ is the domain size:

$$\xi = \frac{2\pi}{w_s} \tag{9}$$

Using the values from the domain size allowed for the calculation of the number of planes (N_p) inside the domains, where *d* is the distance between the backbones.

$$N_p = \frac{\xi}{d} \tag{10}$$

3. X-RAY RESULTS

3.1 POLY(3-OCTYL-THIOPHENE) BULK SAMPLES

The P3OT bulk sample was received from the supplier in powder form and placed in glass capillaries of 2 millimeters in diameter without any further treatment to perform the x-ray measurements. The sample was measured at room temperature for fifty minutes of data collection and also in a cycle of running temperature. The cycle of temperature was stipulated according to the temperature of the phase transition from the polymer, Table 2.1. The aim of this thermal treatment was to evaluate the influence of the temperature and the phase transition on the polymer structure. The annealing process comprised of heating the sample in an oven until 230 ºC for one hour, to ensure the total phase transition of the sample. Then it was placed in the WAXS equipment to perform the x-ray experiments. The sample was cooled down by the equipment using a temperature controller and its heating system. During the cooling process, the sample was also measured following steps of fifty minutes at each temperature. At high temperatures, from 220 to 150 ºC, the sample was measured with 10 ºC intervals, in a total of eight steps. After 150 ºC, steps of 20 ºC were applied until 30 ºC. The whole process lasted around 12.5 hours with a total of 15 steps. The thermal treatment had a higher number of steps at high temperatures to enable an accurate measurement of the phase transition.

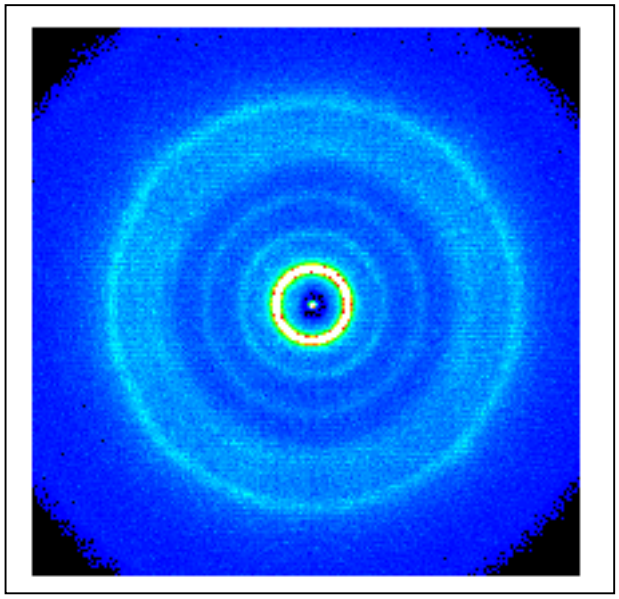

Figure: 3.1: 2D diffraction pattern P3OT bulk sample

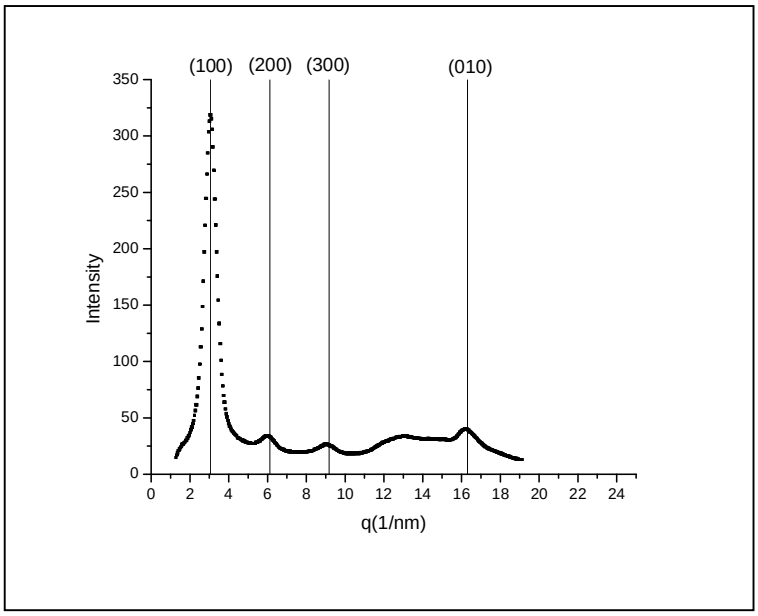

Figure 3.2: Diffraction pattern of P3OT bulk sample at room temperature

The sample showed a typical x-ray diffraction pattern (Figure 3.1), of an isotropic structure, with a circular diffraction pattern coming from a semi-crystalline structure, which contains many crystallites orientated in all directions with equal probabilities.

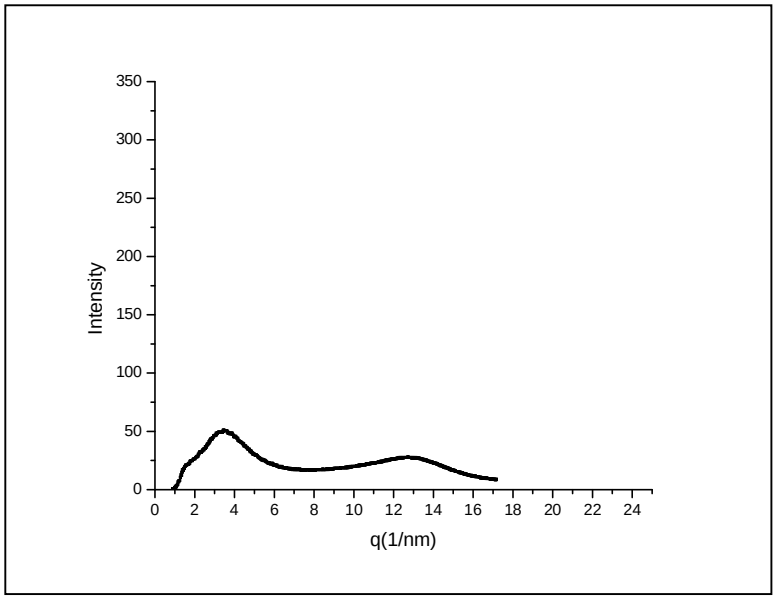

Figure 3.3: Diffraction pattern of P3OT bulk sample at 220 ºC

The diffraction pattern of the P3OT regioregular bulk sample at room temperature, Figure 3.2, showed a well defined peak at low q* range (3.05 nm^{-1}). This peak can be identified as coming from the distance between the polythiophene backbone, related to the distance *a* from the unit cell, Figure 1.3. The two following peaks can be related to the second and the third order from the same distance as the first peak at 5.93 nm^{-1} and 9.0 nm^{-1}, respectively. They are associated to the distance from the closer neighbor's backbone, meaning a high order in a short range. The peak at high q* range (16.3 nm^{-1}) is identified as coming from the π-π stacking of the backbones and related to the distance *b* of the unit cell, Figure 1.3 [5, 16]. In the case of P3OT bulk sample, the octyl side chains have an amorphous conformation explained by the elevation of the intensity between the third order peak and the peak coming from the π-π stacking.

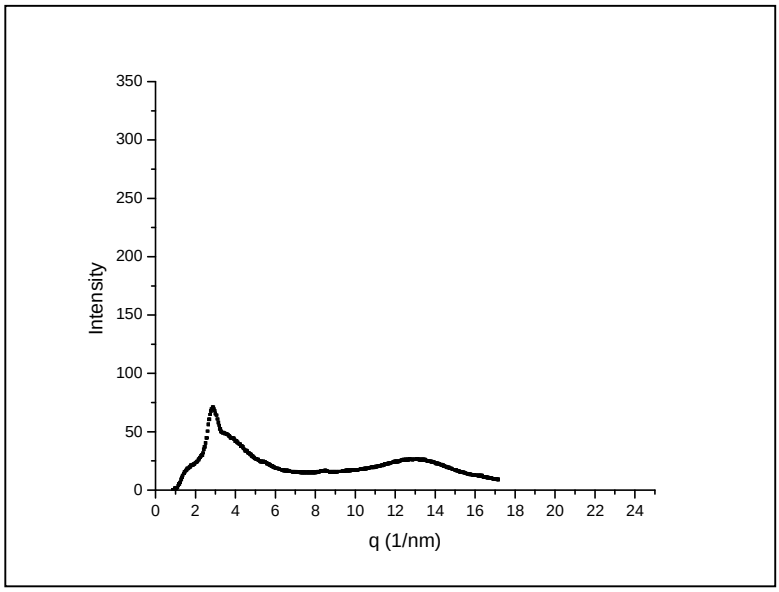

Figure 3.4: Diffraction pattern of P3OT bulk sample at 170 ºC

After heating at 230 °C, the sample showed its phase transition. As observed in the Figure 3.3, the diffraction at 220 ºC showed two broad and low intensity amorphous peaks, meaning that the sample does not have a high ordered structure anymore, with the lamellas showing a random configuration with an indistinct distance between the molecular plans. With the decrease of the temperature, the crystallinity of the sample was increased. The transition amorphous-crystalline can be observed at 170 °C, Figure 3.4. This graph shows the rise of the first order peak at low q range and the decrease of the amorphous halo. The cooling process of the sample was characterized by the decrease of the amorphous peaks followed by

a slight decrease of the distances between the molecular plans from the structure, showed in Table 3.1. Back to room temperature, the structure of the sample became crystalline again with a similar diffraction pattern before the thermal treatment, Figure 3.5. The inter chain distances had no significant changes, even showing a tendency of increasing these distances during the heating of the sample, taking into account the errors from the measurements, Table 3.4. The domain sizes had only a slight increase at the end of the measurements, which is also not significant because of the error from the measurements.

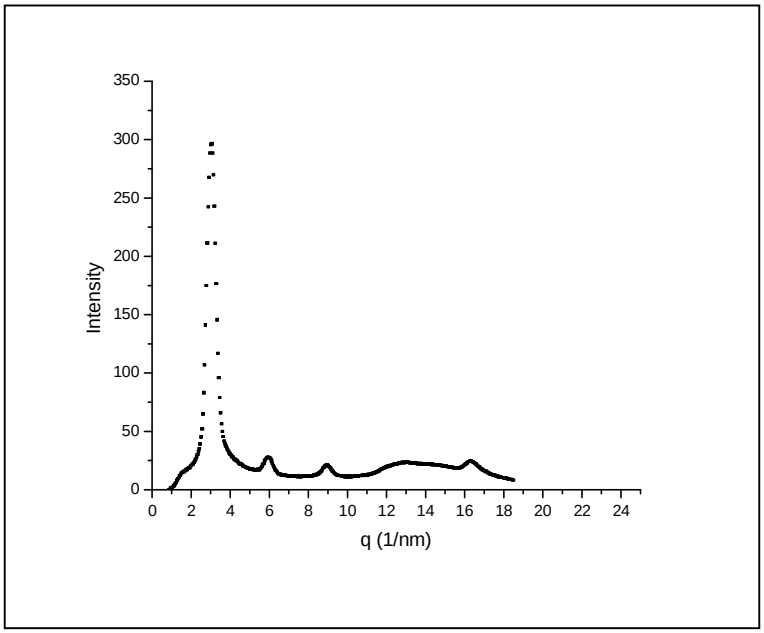

Figure 3.5: Diffraction pattern of P3OT bulk sample at 30ºC after annealing

Table 3.1: d-spacing values of the P3OT bulk samples from the running cycle of temperature

Temperature(ºC)	***(100)(nm) ±0.07***	***(200)(nm) ±0.04***	***(300)(nm) ±0.03***	***(010(nm) ±0.02***	***First Amorphous Peak (nm)±0.06***	***Second Amorphous Peak (nm)±0.03***
Room temperature	2.05	1.06	0.70	0.38	-	-
220	-	-	-	-	1.79	0.50
210	-	-	-	-	1.79	0.49
200	-	-		-	1.79	0.49
190	-	-	-	-	1.79	0.49
180	-	-	-	-	1.79	0.49
170	2.16	1.19	0.74	-	-	-
160	2.19	1.14	0.74	0.38	-	-
150	2.19	1.13	0.74	0.39	-	-
130	2.18	1.12	0.74	0.38	-	-
110	2.16	1.11	0.74	0.38	-	-
90	2.14	1.10	0.73	0.38	-	-
70	2.12	1.09	0.72	0.38	-	-
50	2.09	1.07	0.71	0.38	-	-
30 after annealing	2.07	1.06	0.70	0.38	-	-

3.2. POLY(3-OCTYL-THIOPHENE) FILM SAMPLES

The procedure applied in the measurement of the films had to be varied from the bulk sample. The stacked film samples, after the removal of the “fishing holder”, were placed in a brass holder instead of a glass capillary. Since they showed a low thickness (around 20 µm), the sample needed a longer period of data collection than the bulk sample, in this case two hours. Thus, consistent statistics from the diffraction plans were achieved.

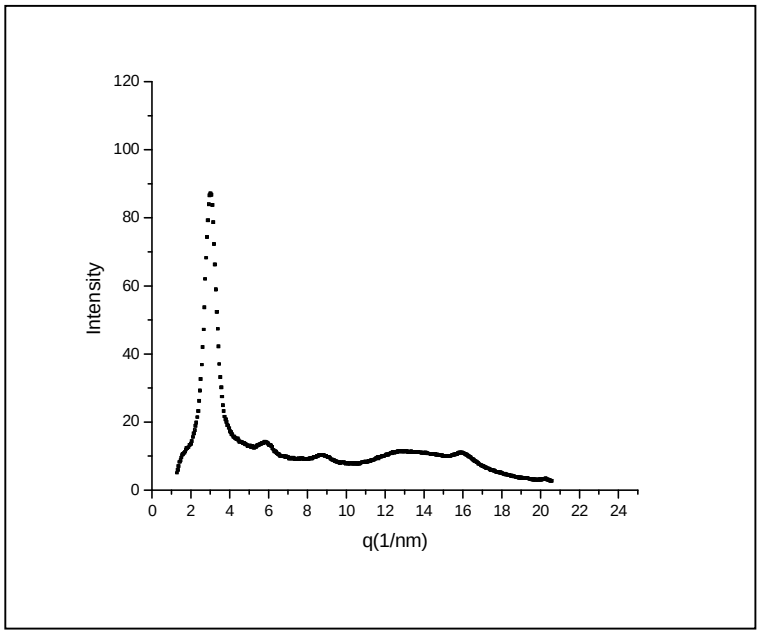

Figure 3.6: Diffraction pattern of P3OT film spun at 4,16 Hz from chloroform

The films were prepared varying the rotational speed and the cast solvent of the preparation procedure. The rotational speed applied in the spin coating process was 4,16 and 33,33 Hz. The solvents were chloroform and chlorobenzene, a total of four samples were produced. The P3OT films did not show a diffraction pattern with severe changes from the bulk pattern, characterized by isotropic structure and the domains randomly orientated. One can see the first three peaks from the first, second and third order of the distances between the backbone as well as the peak related to the π-π stacking at high q range.

The diffraction patterns from all the four samples, Figures 3.6, 3.7, 3.8, 3.9, showed a low intensity for the peak related to the π-π stacking, meaning that only a small number of lamellas were aligned perpendicular to the substrate plan. The high number of lamellas aligned parallel to the substrate plan results in a structure organized in a plan-on

conformation. The relation between the height of the first order peak from the *a* distances and the peak from the *b* distances was kept the same for all the samples, having only a slight change that is not significant. It demonstrates the tendency that the P3OT films have to crystallize in a plan-on configuration is stronger than the influence from the rotational speed and the solvent evaporation rate of the film production process.

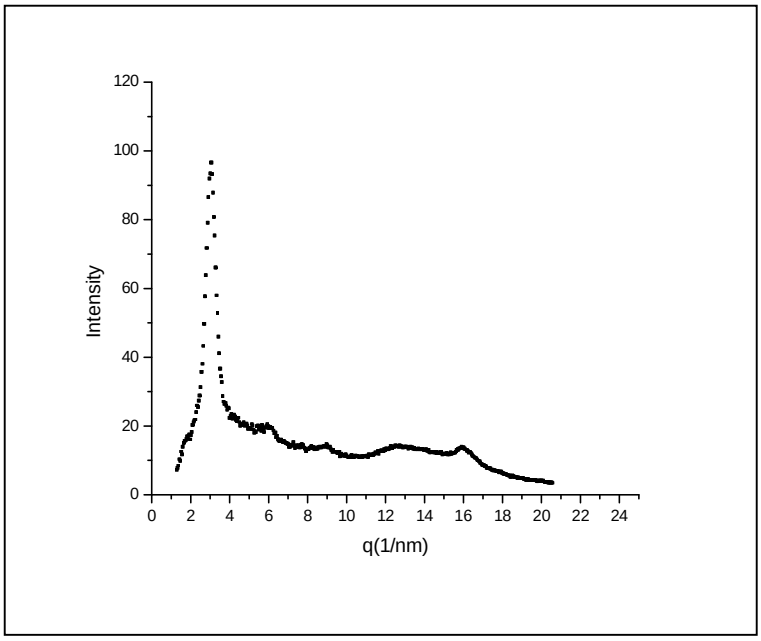

Figure 3.7: Diffraction pattern of P3OT film spun at 4,16 Hz from chlorobenzene

The change of the inter chain distances, showed in Table 3.2, is lower than the error of the measurements, thus the influence of the film preparation is not considered significant and all the values are in accordance with the literature [(5)].

The two samples spun with 4,16 Hz were also measured in a running temperature cycle, which was based on the temperature cycle from the bulk sample. However, due to the longer measuring time of the film experiments, the number of steps had to be decreased. The cycle started at room temperature and had the temperature increased, using the heating system of the equipment and a temperature controller. The cycle of temperature from the film samples were measured in increasing temperature because in contrast to the bulk samples, the films had a known historical treatment caused by the film preparation. After measuring at room temperature, the P3OT films were measured at 150 ºC, taking 10 ºC intervals, the maximum measured temperature was 190 ºC. The last step was at 30 ºC, resulting in seven steps measured in a total of fourteen hours.

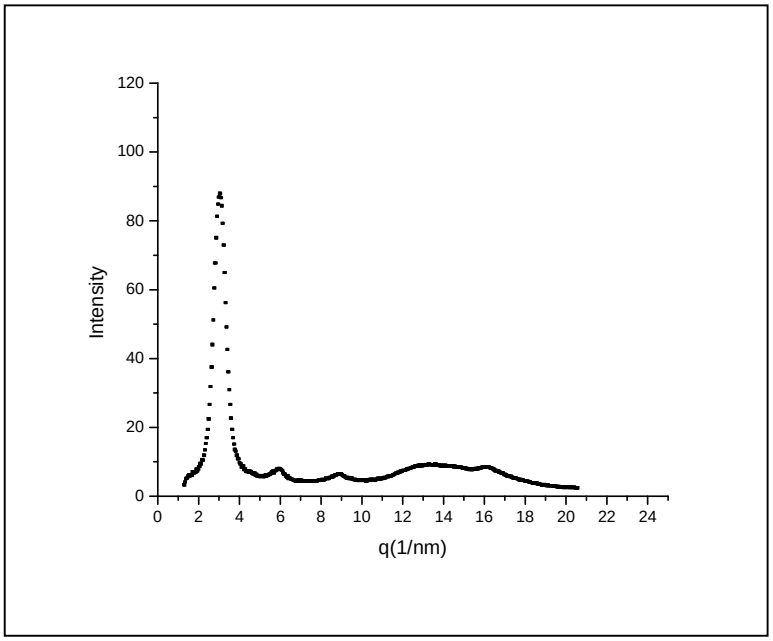

Figure 3.8: Diffraction pattern of P3OT film spun at 33,33 Hz from chloroform

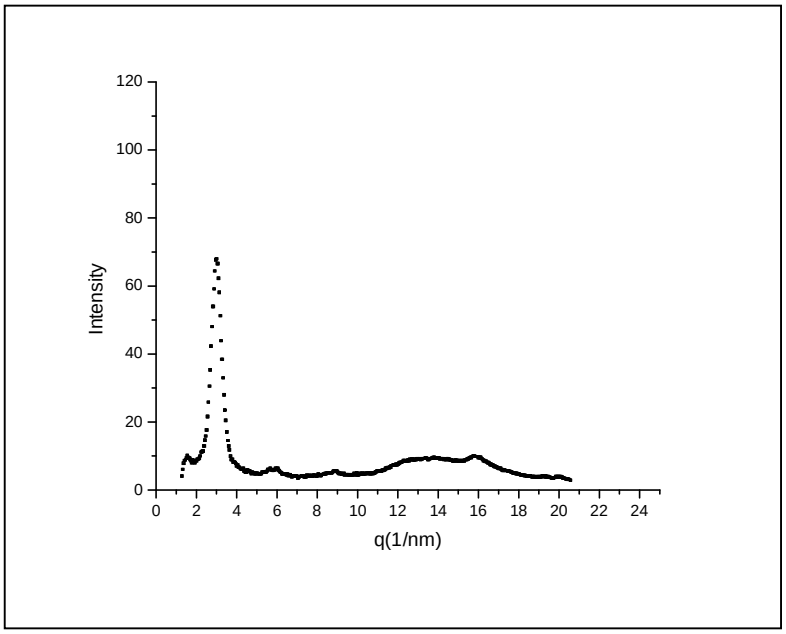

Figure 3.9: Diffraction pattern of P3OT film spun at 33,33 Hz from chlorobenzene

Observing the values for d-spacing calculated from the sample during the thermal treatment, Table 3.3, one can notice the tendency of increasing the d-spacing with the temperature. However taking the error from the measurements into consideration, this

increase is not significant. Contrary to the bulk samples, the films did not showed the phase transition.

Table 3.2: d-spacing values of the P3OT film and bulk samples

	Solvent/Temperature	***(100)(nm) ±0.07***	***(200)(nm) ±0.04***	***(300)(nm) ±0.03***	***(010)(nm) ±0.02***
Bulk	*Room temperature*	2.05	1.06	0.70	0.38
	30ºC after annealing	2.07	1.06	0.70	0.38
4,16 Hz	*Chloroform*	2.09	1.09	0.72	0.39
	Chlorobenzene	2.07	1.09	0.71	0.39
33,33 Hz	*Chloroform*	2.07	1.07	0.71	0.38
	Chlorobenzene	2.09	1.09	0.71	0.39

Table 3.3: d-spacing values of the P3OT films spun at 250 rpm from the running cycle of temperature

	Temperature(ºC)	***(100)(nm)±0.07***	***(200)(nm)±0.04***	***(300)(nm)±0.03***	***(010)(nm)±0.02***
Chloroform	*Room temperature*	2.09	1.09	0.72	0.39
	150	2.19	1.13	0.75	0.39
	160	2.20	1.13	0.75	0.39
	170	2.20	1.14	0.75	0.39
	180	2.21	1.14	0.75	0.39
	190	2.21	1.15	0.76	0.39
	30 after annealing	2.08	1.07	0.71	0.39
Chlorobenzene	*Room temperature*	2.07	1.09	0.71	0.39
	150	2.19	1.13	0.75	0.39
	160	2.20	1.13	0.75	0.39
	170	2.21	1.14	0.75	0.39
	180	2.21	1.15	0.75	0.39
	190	2.22	1.15	0.76	0.39
	30 after annealing	2.08	1.07	0.70	0.39

The domain size of the sample P3OT was calculated for all the films using different preparation and also for the bulk sample before and after the thermal treatment. These values are shown in Table 3.4. The difference between the values from the domain sizes comparing the cast solvent and the rotational speed are not significant. Taking into account the errors from the measurements, the influence of the thermal treatment is also not significant.

The P3OT films were also measured by transmission electron microscopy. Even though the sample showed high beam sensitivity, it was possible to measure the lattice spacing of 0.38 nm for the sample spun at 4.16 Hz from chlorobenzene, Figure 3.10, which is related to the stacking distance from the backbone. The same sample also showed a domain size below 15 nm. The sample spun at 33.33 Hz showed a lattice spacing of 2.0 nm, which is related to the distance between the backbones. All the values measured by the transmission

electronic microscopy were in accordance with the values calculated by the x-ray scattering, which confirm the precision of the x-ray measurements of the staked film samples.

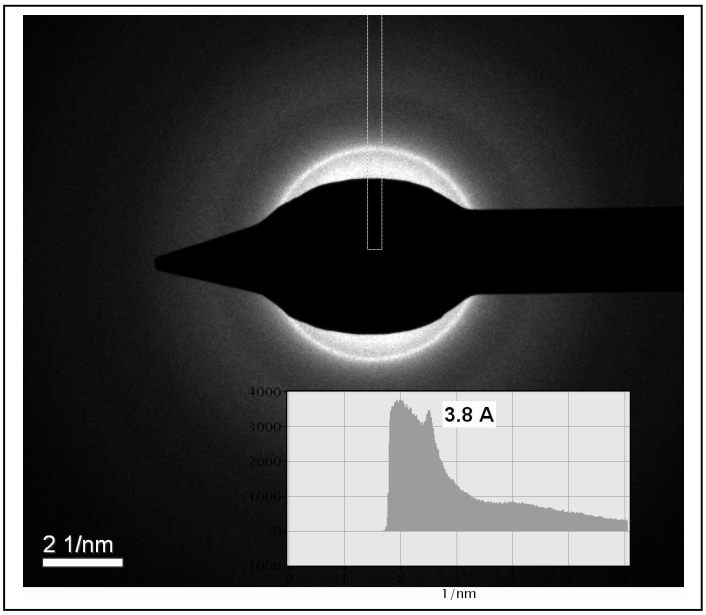

Figure 3.10: Transmission electronic microcopy picture from the P3OT film sample spun at 4.16 Hz from chlorobenzene

Table 3.3: domain size values of the P3OT film and bulk samples

	Solvent/Temperature	***Full width at Half max. (1/nm)***	***Domain Size (nm)***	***Number of Plans***
Bulk	*Room temperature*	0.55±0.06	11.3±1.2	5±1
	30ºC after annealing.	0.36±0.09	17.3±4.4	8±2.5
4,16 Hz	*Chloroform*	0.66±0.06	9.5±0.8	4±0.8
	Chlorobenzene	0.54±0.07	11.7±1.5	6±1.1
33,33 Hz	*Chloroform*	0.64±0.05	10.0±0.8	5±0.8
	Chlorobenzene	0.48±0.07	13.0±1.8	6±1.3

3.3. POLY(3-HEXYL-THIOPHENE) BULK SAMPLE

Following a similar procedure from P3OT, the P3HT bulk sample was measured at room temperature without any previous treatment. The time of data collection was fifty minutes for all measurements. Although the samples showed different temperature of phase transition, the running temperature cycle was similar. The maximum temperature reached by the heating system of the WAXS equipment was 220 ºC, which was lower than the temperature at the end of the phase transition for P3HT, Table 2.1. Before running the

temperature cycle, the sample was heated in an oven for one hour at 260 ºC. Then the sample was placed in the WAXS equipment at 220 ºC to continue the thermal treatment. The sample was cooled down by the equipment using a temperature controller and its heating system. At high temperatures, from 220 to 150 ºC, the sample was measured with 10 ºC steps, in a total of eight steps. After 150 ºC, steps of 30 ºC were applied until 30 ºC. The whole process lasted almost 11 hours with a total of 15 steps. The thermal treatment had a higher number of steps at high temperatures to enable an accurate measurement of the phase transition.

The sample showed a typical x-ray diffraction pattern (Figure 3.11), of an isotropic structure, with a circular diffraction pattern coming from a semi-crystalline structure, which contains many crystallites orientated in all directions with equal probabilities.

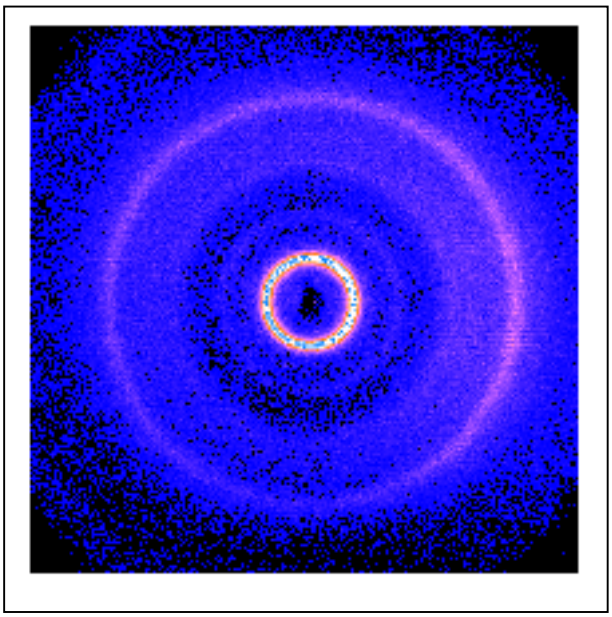

Figure 3.11: 2D diffraction pattern of P3OT bulk sample

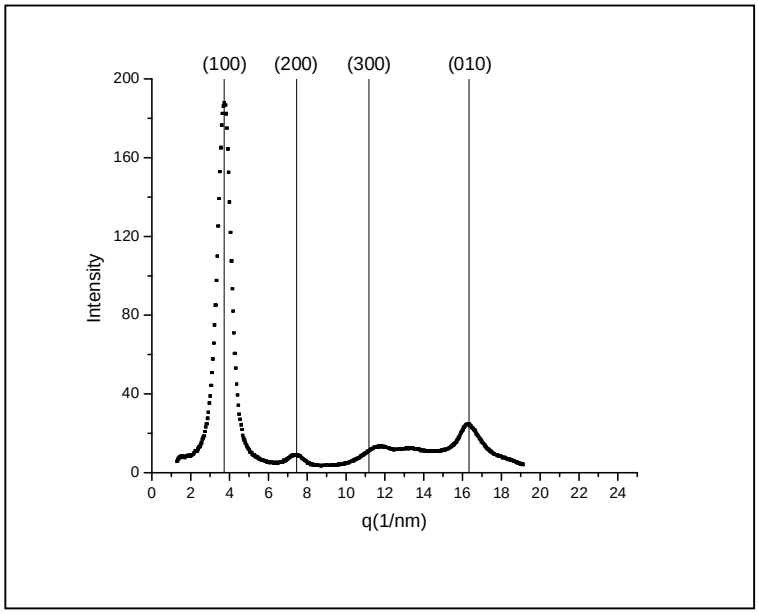

Figure 3.12 Diffraction pattern of P3HT sample at room temperature

The diffraction pattern of the P3HT bulk sample at room temperature, Figure 3.12 showed a well defined peak at low q* range (3.72 nm^{-1}), which can be identified as the diffraction peak of the first order from the distance between the lamellas and related to the *a* distance from the unit cell (Figure 1.3). The following peak is related to the second order diffraction at 7.36 nm^{-1}, which represents the diffraction from the neighbor's backbones in the same direction. The third peak at 11.65 nm^{-1} could also be interpreted as the third order one, but it presents a small shift to a higher value of q*. The peak at high q* range (16.33 nm^{-1}) is identified as coming from the π-π stacking and related to the distance b of the unit cell [(5)], Figure 1.3. As expected, the distance between the lamellas from the P3HT samples (1.65 nm) are smaller than the distance from the P3OT samples (2.09 nm).

The lamellas of the polythiophene are separated by the side chains attached to the back bone of the polymer, thus the addition of an octyl side chain results in a larger distance between the lamellas than the addition of a hexyl side chain, see Tables 3.1 and 3.5. In the case of P3HT bulk sample, the hexyl side chains have an amorphous conformation explained by the elevation of the intensity between the third order peak and the peak coming from the π-π stacking.

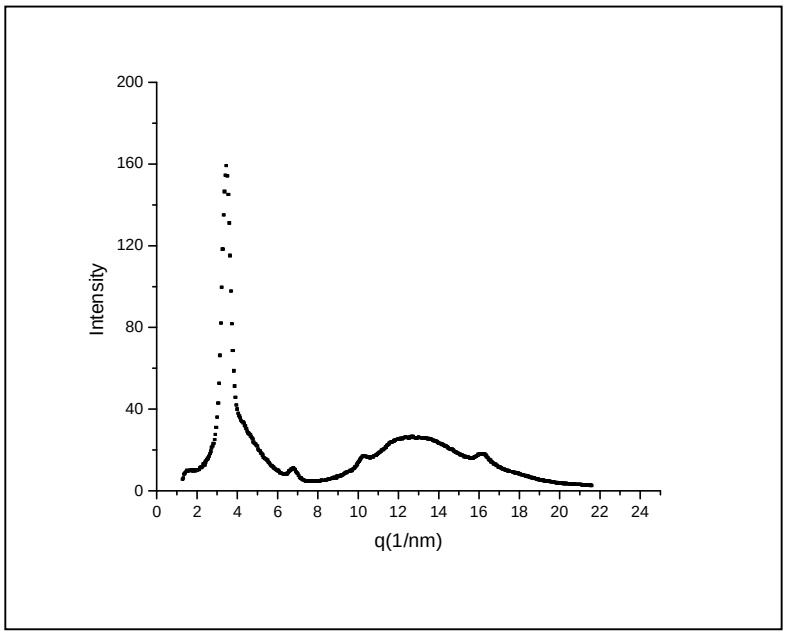

Figure 3.13: Diffraction pattern of P3HT sample at 220 ºC

As explained before, the measurement of the phase transition from the P3HT was limited by the working temperature of the WAXS equipment. Thus this transition could not be observed. Even after heating the sample over the temperature of phase transition. The thermal treatment increased the amorphous character of the structure. The Figure 3.13 shows the broadening from the base of the peaks and the decrease of their intensities. Surprisingly, during the cooling of the sample, the structure, instead of returning to the original conformation, it had its amorphous character increased, characterized by the decrease of the intensity and the broadening of the peaks, Figures 3.14 and 3.15. GPC measurements were performed with the samples after the annealing process, but the polymer could not get into solution and be measured by the equipment. Thus this sample probably suffered a crosslink between the backbones, which did not allow the structure to return to the original conformation.

Increasing the temperature, the sample showed a tendency towards normal thermal expansion, resulting in an increase of the inter chain stacking, Table 3.5. However, taking into consideration the errors from the measurements, these changes are not significant. Some of the peaks were not able to be calculated during the “cooling” of the material because of the broadening of peaks, which made the deconvolution of the peaks impossible for the software.

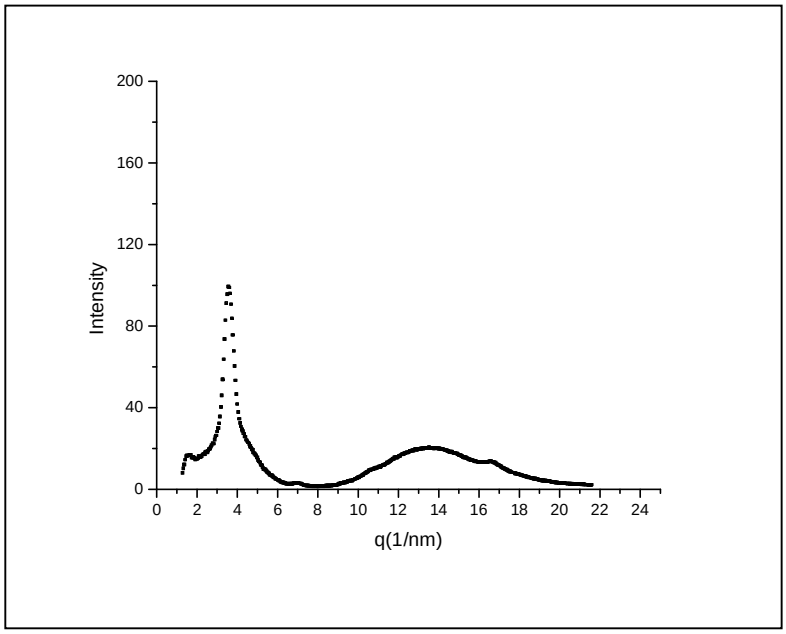

Figure 3.14: Diffraction pattern of P3HT sample at 150 ºC

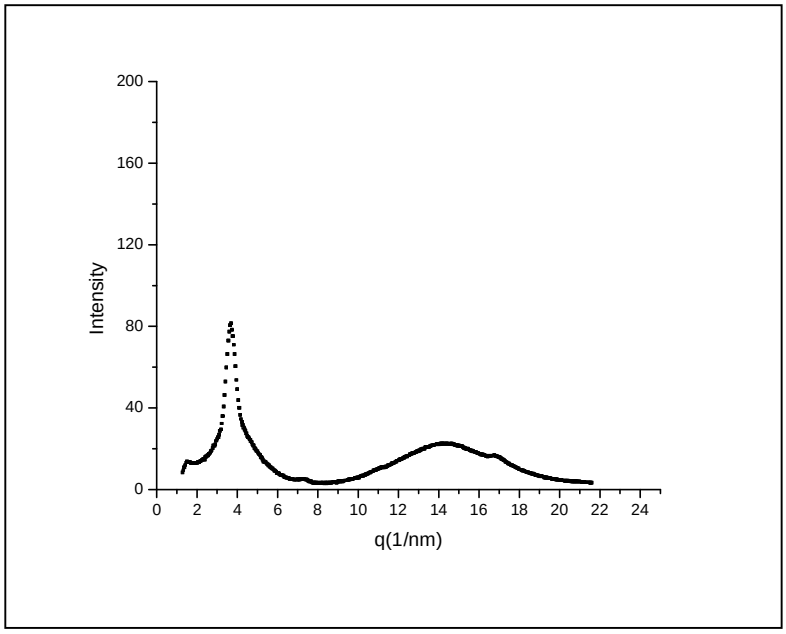

Figure 3.15: Diffraction pattern of P3HT sample at 30 ºC after annealing

Table 3.5: d-spacing values of the P3HT bulk samples from the running cycle of temperature

Temperature(ºC)	*(100)(nm)±0.06*	*(200) (nm)±0.03*	*(300) (nm)±0.02*	*(010) (nm)±0.02*
Room temperature	1.69	0.85	0.54	0.38
220	1.81	0.93	0.60	0.39
210	1.81	0.93	0.60	0.39
200	1.80	0.92	0.60	0.38
190	1.79	0.92	0.59	0.38
180	1.78	0.91	0.58	0.38
170	1.77	0.91	0.58	0.38
160	1.76	0.91	0.56	0.38
150	1.75	0.91	-	0.38
120	1.74	0.89	-	0.38
90	1.73	0.89	-	0.38
60	1.71	0.88	-	0.38
30 after annealing	1.70	0.87	-	0.38

3.4. POLY(3-HEXYL-THIOPHENE) FILM SAMPLES

The measurements of the P3HT films focused on the investigation of three parameters: the rotational speed (4,16 and 33,33 Hz), the solvent (chloroform and chlorobenzene) and the surface of the substrate (hydrophobic and hydrophilic). This led to a total of six different samples. All samples were measured at room temperature for two hours of data collection and using a brass holder to place the sample in the equipment.

The samples showed the same diffraction peaks as the bulk sample. Different from the P3OT films, the P3HT films showed a strong influence from the varying parameters, especially the samples spun with 4,16 Hz on hydrophilic treatment, Figure 3.16 and 3.17. High intensity of the diffraction peak is observed from the π-π stacking, meaning that the film has a high number of planes aligning perpendicular to the substrate, which is typical of an edge-on conformation. In the films cast from chlorobenzene, Figure 3.17, the edge-on character is higher than the films cast from chloroform, Figure 3.16, due to the higher intensity of the peak coming from π-π stacking in comparison to the peak coming from the distance between the backbones. This observation can be explained by the longer time for the organization of the molecules given by the low evaporation rate of the chlorobenzene.

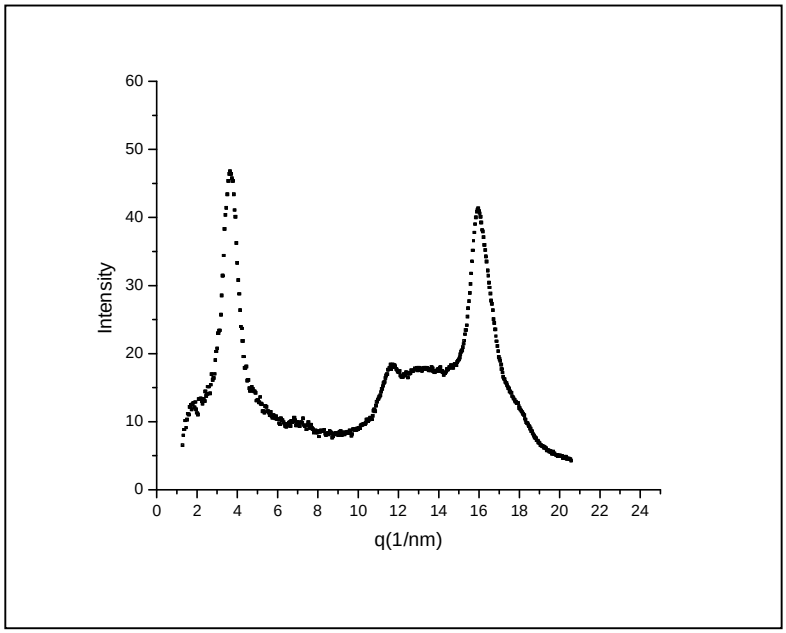

Figure 3.16: Diffraction pattern of P3HT film spun at 4,16 Hz from chloroform

The P3HT films have a tendency to crystallize in edge-on conformation. However, by increasing the rotational speed, this character is decreased, as seen in the Figures 3.18 and 3.19 from the films spun with 33.33 Hz. In these graphs, the peaks coming from the π-π stacking showed a decrease in the intensity, which means that the film has a lower quantity of planes aligned perpendicular to the substrate than the films spun at 4.16 Hz. This result can be explained by the increase of the evaporation rate caused by the increase of the rotational speed in the process. A fast evaporation allow less time for the lamellas to organize themselves in a conformation close to the equilibrium. As showed by the films spun at 4,16 Hz, the 33,33 Hz film cast from chlorobenzene also showed an increasing trend of the edge-on orientation in comparison to the films from chloroform.

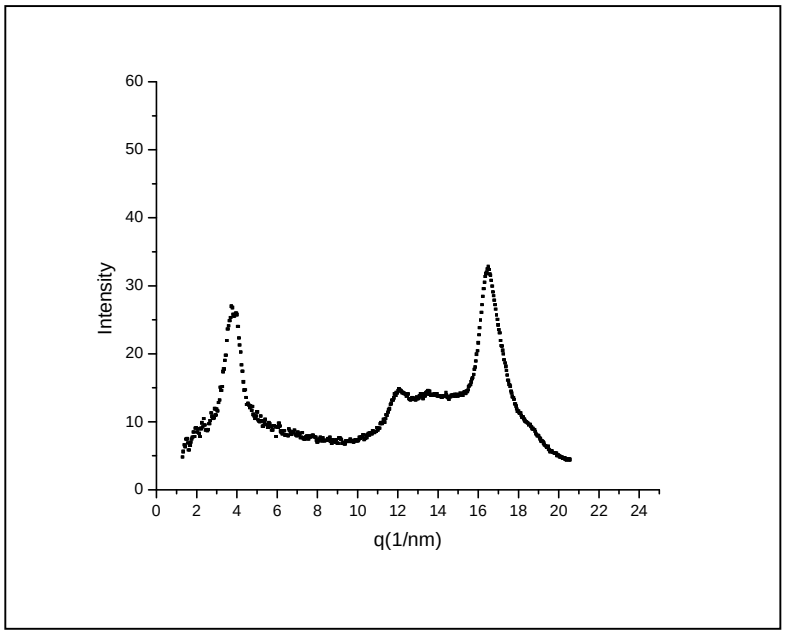

Figure 3.17: Diffraction pattern of P3HT film spun at 4,16 Hz from chlorobenzene

As described in Section 1.1.6, the surface has a strong influence on the crystallization of the films. Studies [20] were already made on films spun on a hydrophobic surface; they showed that a hydrophobic treatment improves the charge mobility of the PAT films. Due to this influence on the electrical properties, films spun on a hydrophobic surface treated with HMDS were prepared to identify the structural changes caused by the surface. P3HT films were cast from chloroform and chlorobenzene using a rotational speed of 4,16 Hz. The Figures 3.20 and 3.21 show the diffraction peaks from the two films prepared on a hydrophobic surface. One can see that the peak at (16.33 nm^{-1}) coming from the π-π stacking showed a lower intensity than the films spun on a hydrophilic surface, which results in a lower edge-on tendency for the films from a hydrophobic surface.

This result showed a decrease of the edge on orientation for the films spun on a hydrophobic surface, which is in contradiction with the results from the electronic properties experiments. The edge-on conformation increases the charge mobility of the films [11] and the films spun on a hydrophobic surface also showed higher charge mobility than the films spun on a hydrophilic surface [20]. However, x-ray measurements are limited to explain such observations because the influence of the surface only plays an important role on the molecules close to the surface. AFM experiments showed that the hydrophobic treatment changes the morphology of the films close to the surface of the substrate, exactly were it is more relevant for the charge mobility.

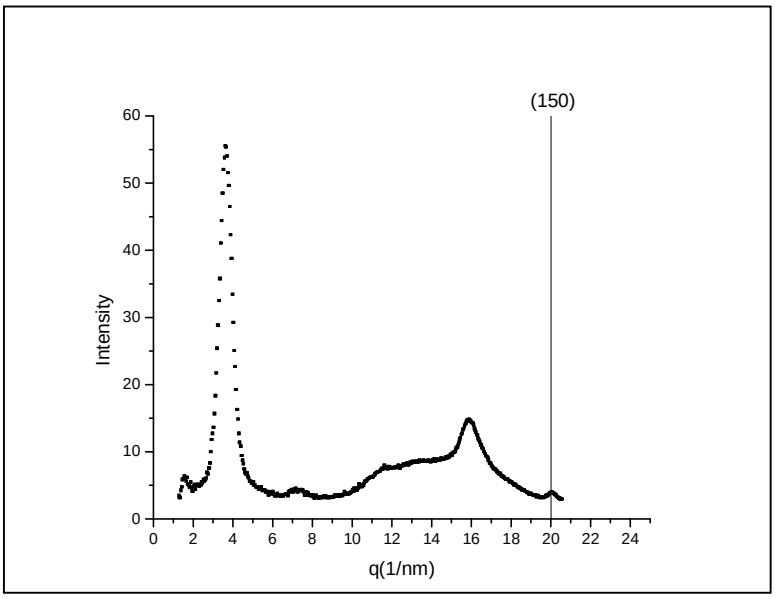

Figure 3.18: Diffraction pattern of P3HT film spun at 33,33 Hz from chloroform

The graphs from the samples spun at 33,33 Hz, Figures 3.18 and 3.19, and from the samples at 4,16 Hz on HMDS surface, Figure 3.20 and 3.21, showed a peak at 19.5 nm^{-1}, which was calculated as coming from the (150) plane. The identification of this peak results in high order in long range of the film because it comes from a plane made by molecules relatively distant from each other. In the case of the samples from 4,16 Hz, this peak has a higher intensity because it has a high order than the films from 33,33 Hz. This is explained by the longer time given by the low rotational speed for the molecules to organize.

The change of the inter chain distances, showed in Table 3.7, is lower than error of the measurements, thus the influence of the film preparation is not considered significant and all the values are in accordance with the literature [(5)].

The films spun with 4,16 Hz on hydrophilic surface were also measured on a running temperature cycle, as was performed with the P3OT films. The cycle was made with an increasing of temperature. The temperatures were determined according to the phase transition of the P3HT bulk sample, Table 2.1. The first step after the room temperature measurement was made at 180 ºC; using 10 ºC intervals, the highest temperature reached by the equipment was 220 ºC. The last measurement was again performed at 30 ºC, with a total of six different temperatures measured within twelve hours of the experiment.

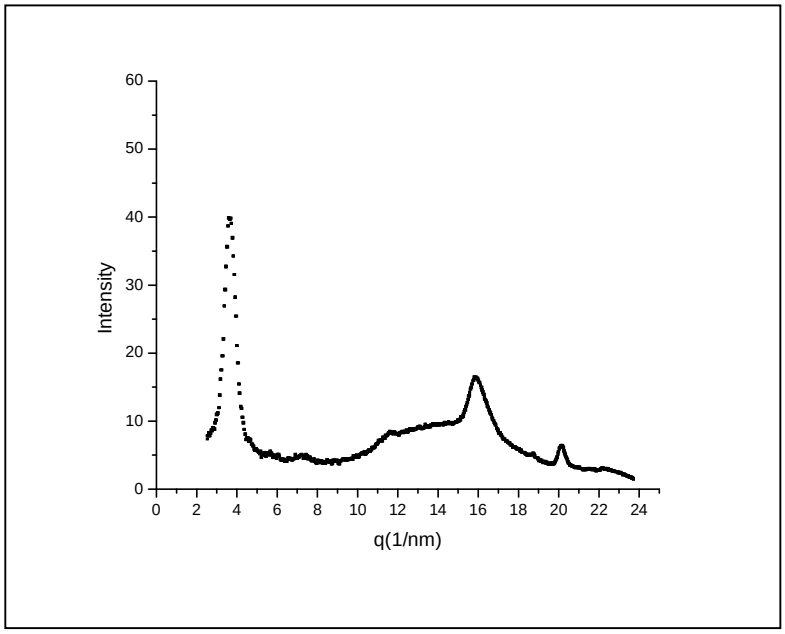

Figure 3.19: Diffraction pattern of P3HT film spun at 33,33 Hz from chlorobenzene

The phase transition for the P3HT was also not observed. Increasing the temperature, the sample showed a tendency towards normal thermal expansion, resulting in an increase of the inter chain stacking, Table 4.6. However, taking into consideration the errors from the measurements these changes are not significant. Some of the peaks were not able to be calculated during the "cooling" of the material because of the broadening of peaks, which made the deconvolution of the peaks not possible for the software

Table 3.6: d-spacing values of the P3HT films spun at 250 rpm from the running cycle of temperature

	Temperature(ºC)	***(100)(nm)±0.06***	***(200)(nm)±0.03***	***(300(nm)±0.02***	***(010)(nm)±0.02***
Chloroform	*Room temperature*	1.72	0.92	0.53	0.39
	180	1.84	0.94	0.54	0.39
	190	1.84	0.93	0.54	0.39
	200	1.83	0.94	0.54	0.39
	210	1.83	0.95	0.53	0.39
	220	1.81	-	0.51	0.39
	30 after annealing	1.72	-	-	0.38
Chlorobenzene	*Room temperature*	1.65	-	0.52	0.38
	180	1.83	-	0.53	0.39
	190	1.83	-	0.53	0.39
	200	1.84	-	0.53	0.39
	210	1.84	-	0.53	0.39
	220	1.83	-	0.51	0.39
	30 after annealing	1.73	-	-	0.39

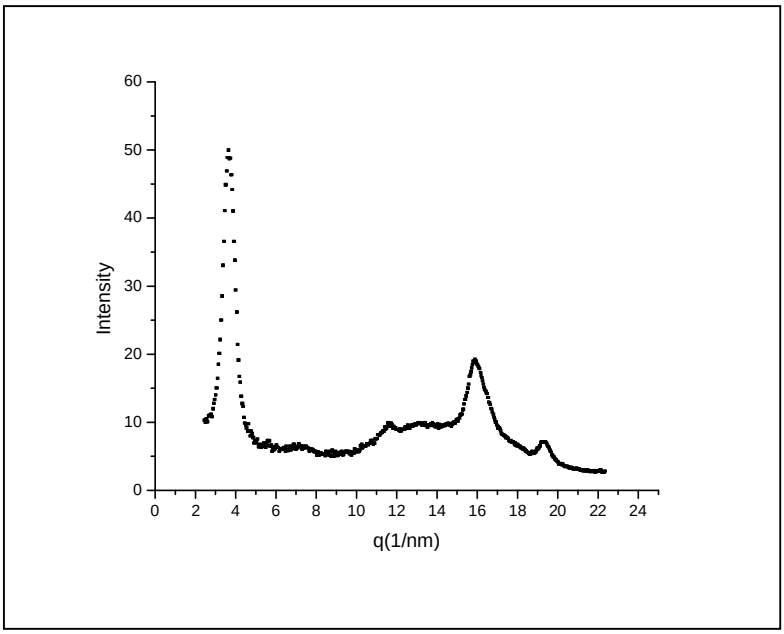

Figure 3.20: Diffraction pattern of P3HT film spun at 4,16 Hz from chloroform on HMDS surface

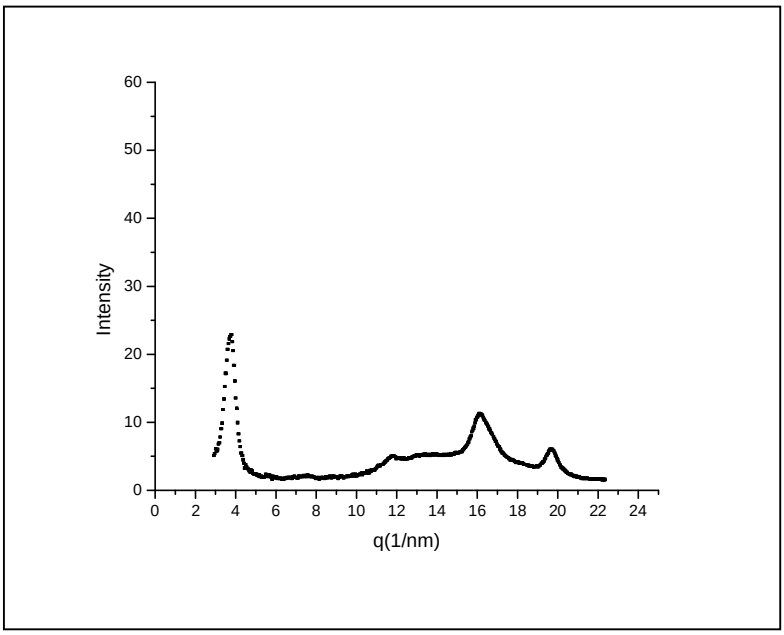

Figure 3.21: Diffraction pattern of P3HT film spun at 4,16 Hz from chlorobenzene on HMDS surface

The films spun at 4,16 Hz on a hydrophilic surface were also measured by the XRD technique. The diffraction pattern, Figures 3.22 and 3.23, showed the same peaks as the 2D WAXS technique showed. The difference is the intensity of the peak coming from the

distance *b*, which had a much lower intensity compared to the peak coming from the distance *a* in the pattern measured by the XRD equipment. Because this technique probes structures parallel to the surface, the low intensity of this peak means that most of the planes of the film are aligned perpendicular to the substrate, resulting in an edge-on conformation. These measurements were a confirmation of the results from the 2D WAXS technique.

Observing the values of the d-spacing calculated from the diffraction peaks of the P3HT films, Table 3.7, affirms that the rotational speed, the cast solvent and the surface have no significant influence on the inter chain stacking. Even for the measurements from XRD, which has a higher resolution, the influence of the rotational speed is also not significant.

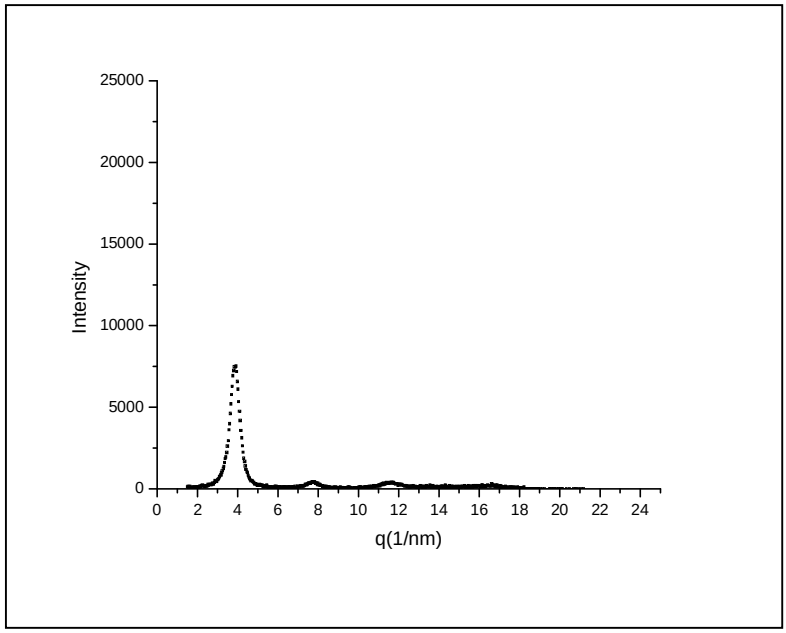

Figure 3.22: XRD diffraction pattern of P3HT film spun at 4,16 Hz from chloroform

Table 3.7: d-spacing values of the P3OT film and bulk samples measured by 2D WAXS

	Solvent/Temperature	***(100)(nm) ±0.06***	***(200)(nm) ±0.03***	***(300(nm) ±0.02***	***(010)(nm) ±0.02***	***(150(nm) ±0.01***
Bulk	*Room temperature*	1.68	0.85	0.54	0.38	-
	30ºC after annealing	1.70	0.87	-	0.38	-
4,16 Hz	*Chloroform*	1.72	0.92	0.53	0.39	-
	Chlorobenzene	1.65	-	0.52	0.38	-
	Chloroform (HMDS)	1.71	0.88	0.54	0.39	0.32
	Chlorobenzene(HMDS)	1.69	0.84	0.53	0.39	0.32
33,33 Hz	*Chloroform*	1.72	0.87	0.53	0.39	0.31
	Chlorobenzene	1.72	0.88	0.53	0.39	0.31

Table 3.8: d-spacing values of the P3OT film measured by XRD

	Solvent	*(100)(nm) ±0.03*	*(200)(nm) ±0.02*	*(300(nm) ±0.01*	*(010)(nm)*	*(150)(nm) ±0.01*
4,16 Hz	*Chloroform*	1.63	0.81	0.54	-	-
	Chlorobenzene	1.61	0.81	0.54	-	0.30

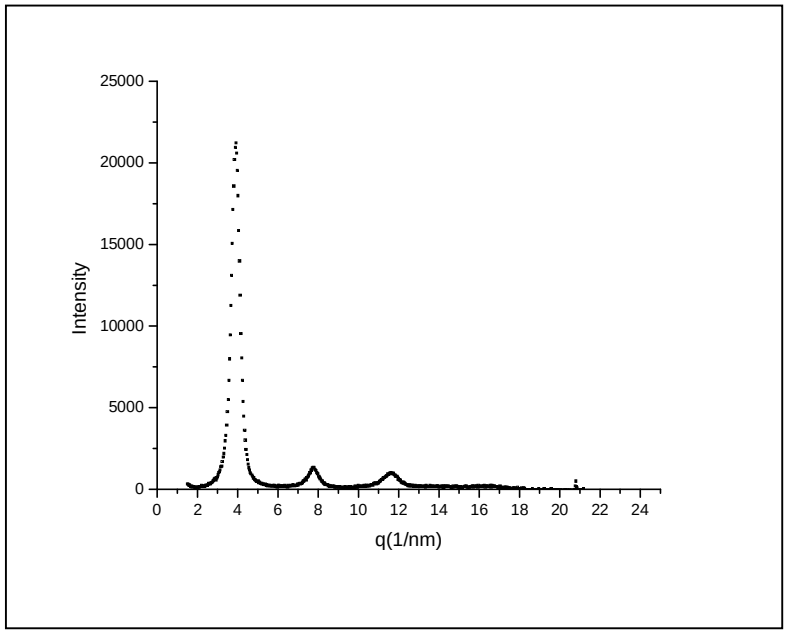

Figure 3.23: XRD diffraction pattern of P3HT film spun at 4,16 Hz from chlorobenzene

The domain size of the sample P3HT was calculated for all the films using different preparation and also for the bulk sample before and after the thermal treatment. These values are shown in Table 3.9. The difference between the values from the domain sizes in comparison to the cast solvent, the rotational speed and the surface are not significant. Taking into account the errors from the measurements; the influence of the thermal treatment is also not significant.

Table 3.9: domain size values of the P3HT film and bulk samples

	Solvent/Temperature	*Full width at Half max. (1/nm)*	*Domain Size (nm)*	*Number of Plans*
Bulk	*Romm temperature*	0.75±0.05	8.3±0.5	5±0.6
	30ºC after anneal.	0.54±0.07	11.6±1.5	7±0.5
4,16 Hz	*Chloroform*	0.87±0.05	7.2±0.5	4±0.5
	Chlorobenzene	1.17±0.09	5.4±0.4	3±0.6
	Chloroform (HMDS)	0.69±0.06	9.1±0.7	5±0.7
	Chlorobenzene (HMDS)	0.81±0.07	7.8±0.7	5±0.6
33,33 Hz	*Chloroform*	0.75±0.05	8.4±0.5	5±0.6
	Chlorobenzene	0.66±0.06	9.6±0.9	6±0.8
XRD	*Chloroform*	0.49±0.02	12.8±0.5	8±0.9
	Chlorobenzene	0.39±0.02	16.2±0.7	10±1.1

3.5. REGIORANDOM SAMPLES

The regiorandom bulk samples from the both polymers, P3HT and P3OT, were also measured by the 2D WAXS equipment. The diffraction patterns are shown in Figures 3.24 and 3.25. Both samples already showed at room temperature an amorphous structure, characterized by the two broad and low intensity diffraction peaks. This means that the sample does not have a high ordered structure, with the lamellas showing a random configuration with an undefined distance between the molecular planes. DSC and TGA were performed with the samples; the measurements did not show any phase transition for the two samples, Table 2.1. The running temperature cycle followed the same cycle for the regioregular samples. The thermal treatment did not show any significant impact on the structure of the regiorandom samples; the inter chain distances and the shape of the peaks were kept the same. Because the regiorandom samples are amorphous, the films spun with a 10mg/ml solution would also have an amorphous structure [(25)]. Thus the film preparation influence would be even lower in this case.

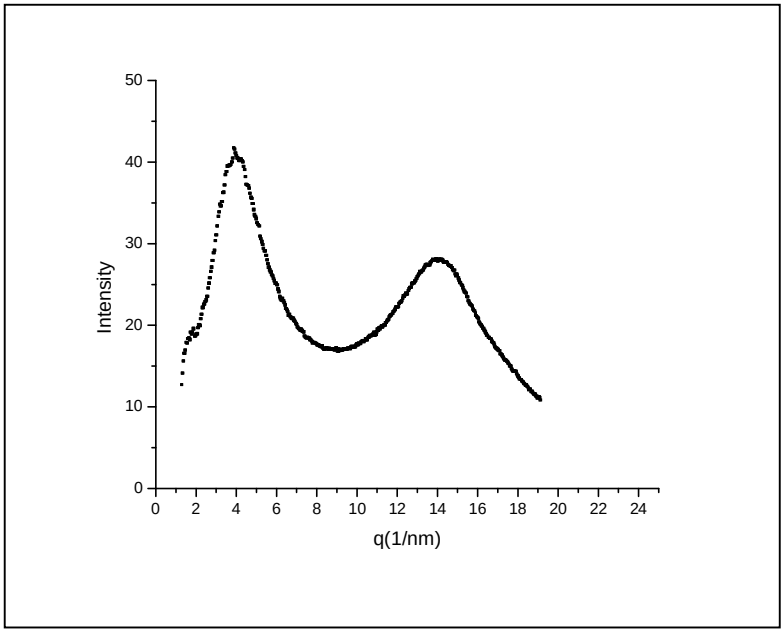

Figure 3.24: Diffraction pattern of P3HT regiorandom bulk sample at room temperature

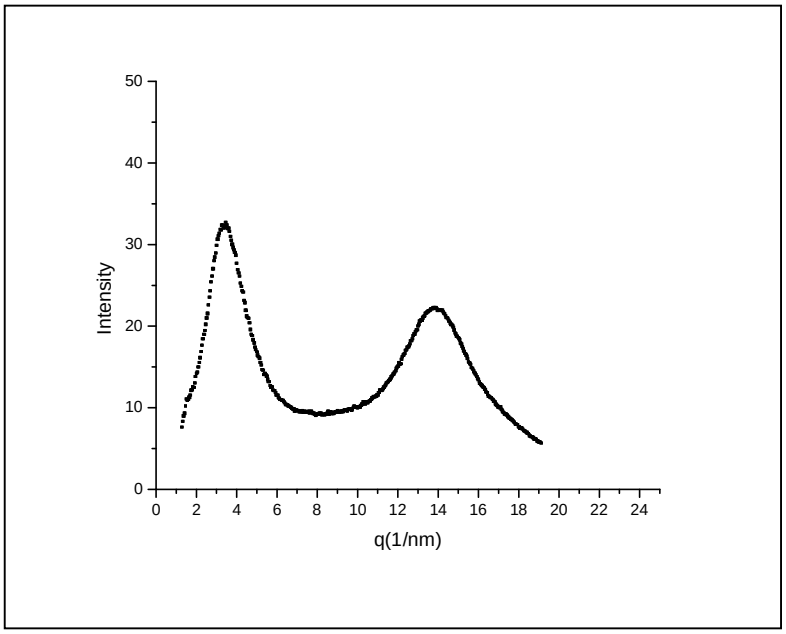

Figure 3.25: Diffraction pattern of P3OT regiorandom bulk sample at room temperature

4. CONCLUSION

The evaluation of the polythiophene structure showed that the film preparation can influence the polymer orientation of the films, resulting also in a variation of the electrical properties. The x-ray measurements of the thin films using an in-house source were a challenge because it was never done before and there were some unclear parameters, which brought difficulties to perform the technique. The important parameters to be determined during the sample preparation were the optimal thickness of the stacked samples and the removal of the films from the substrate without damaging them. After the x-ray measurements, it is concluded that the sample preparation method was successfully performed, allowing all the measurements to be done, without any influence of the sample preparation procedure on the results of the x-ray scattering.

According to the results, it is concluded that the film preparation, regarding the rotational speed, cast solvent and surface character, had no impact on the inter-chain distances and the domain sizes of all the samples. It can be assumed from this that using a film production technique, which works closer to the equilibrium condition like drop casting, the influence of the cast solvent on the domain sizes would be stronger.

The length of the side chains has a high impact on the structure of the film and its orientation. The longer the side chains, the bigger the distances between the backbones, as was shown by comparing the samples P3HT and P3OT. By increasing the length of the side chains, the face-on orientation is enhanced and the influence of the rotational speed and the cast solvent is also decreased, as seen in the results from the P3OT film sample. This sample only showed a small impact from the film preparation on the chain orientation.

The P3HT film samples showed a structure orientation more sensitive to the film preparation condition than the P3OT films. The P3HT films have a tendency to orientate on an edge-on conformation. However, applying film preparation conditions, which are not close to equilibrium conditions, the edge-on orientation was decreased and the face-on orientation was enhanced. In the case of this work, high rotational speed of the spin coating process, high vapor pressure solvent and hydrophobic surface are the parameters that enhance the face-on conformation.

Due to time constraints of the work, the electrical properties of the films could not be measured. This measurement would complete the work, thereby facilitating the improvement of the device production. Studies that evaluate of all the parameters of film preparation and following the same method could not be found. Instead, there are only studies evaluating the

parameter separately, making a comparison complicated. Each study followed a different film preparation methodology while using the same polymer, but from different suppliers. Such variations lead to significant impacts on the results.

Measuring the electrical properties would also show which parameter from the film preparation has a higher impact on the device efficiency; allowing production optimization by focusing on managing the parameter that has a stronger influence on the electrical properties.

REFERENCES

[1] Hu, X. *Polymer* **2000,** *41,* 9147–9154.

[2] Tashiro, K.; Ono, K.; Minagawa, Y.; Kobayashi, M.; Kawai, T.; Yoshino, K. *Journal of Polymer Science Part B: Polymer Physics* **1991,** *29,* 1223–1233.

[3] Kline, J. R.; Mcgehee, M. D.; Kadnikova, E. N.; Liu, J.; Frechet, J. M.; Toney, M. F. *Macromolecules* **2005,** *38,* 3312–3319.

[4] Aasmundtveit, K.; Samuelsen, E.; Mrdalen, J.; Bakken, E.; Carlsen, P.; Lienert, U. *Synthetic Metals* **1997,** *89,* 203–208.

[5] Pal, S.; Nandi, A. K. *Macromolecules* **2003,** *36,* 8426–8432.

[6] Zen, A.; Saphiannikova, M.; Neher, D.; Grenzer, J.; Grigorian, S.; Pietsch, U.; Asawapirom, U.; Janietz, S.; Scherf, U.; Lieberwirth, I.; Wegner, G. *Macromolecules* **2006,** *39,* 2162–2171.

[7] Sirringhaus, H. *Synthetic Metals* **2000,** *111-112,* 129–132.

[8] Joshi, S.; Grigorian, S.; Pietsch, U.; Pingel, P.; Zen, A.; Neher, D.; Scherf, U. *Macromolecules* **2008,** *41,* 6800–6808.

[9] Hao, X. T.; Hosokai, T.; Mitsuo, N.; Kera, S.; Okudaira, K. K.; Mase, K.; Ueno, N. *The Journal of Physical Chemistry B* **2007,** *111,* 10365–10372.

[10] Gurau, M. C.; Delongchamp, D. M.; Vogel, B. M.; Lin, E. K.; Fischer, D. A.; Sambasivan, S.; Richter, L. J. *Langmuir* **2007,** *23,* 834–842.

[11] Delongchamp, D. M.; Vogel, B. M.; Jung, Y.; Gurau, M. C.; Richter, C. A.; Kirillov, O. A.; Obrzut, J.; Fischer, D. A.; Sambasivan, S.; Richter, L. J.; Lin, E. K. *Chemistry of Materials* **2005,** *17,* 5610–5612.

[12] Chang, J.-F.; Sun, B.; Breiby, D. W.; Nielsen, M. M.; Solling, T. I.; Giles, M.; Mcculloch, I.; Sirringhaus, H. *Chemistry of Materials* **2004,** *16,* 4772–4776.

[13] Chabinyc, M. L. *Polymer Reviews* **2008**.

[14] Bao, Z.; Dodabalapur, A.; Lovinger, A. J. *Applied Physics Letters* **1996,** *69,* 4108–4110.

[15] Prosa, T. J.; Winokur, M. J.; Moulton, J.; Smith, P.; Heeger, A. J. *Macromolecules* **1992,** *25,* 4364–4372.

[16] Breiby, D. W.; Samuelsen, E. J. *Journal of Polymer Science Part B: Polymer Physics* **2003,** *41,* 2375–2393.

[17] Brückner, *S.;* Porzio, W. *Mukromol. Chem.* **1989,**89, 961**.**

[18] Gamier, F.; Tourillon, G.; Barraud, J. Y.; Dexpert, H. *J. Mater. Sci.* **1985**, 25, 2687.

[19] Chen, T.-A.; Wu, X.; Rieke, R. D. *J. Am. Chem. Soc.* **1995**, *117*, 233.

[20] Scavia, G; Porzio, W; Destri , S; Barba, L; Arrighetti, G; Milita, S; Fumagalli, L; Natali, D; Sampietro M.; Surface Science **2008,** 602, 3106.

[21] Wikipedia, T. "http://en.wikipedia.org/wiki/Wide_angle_X-ray_scattering", accessed 20/01/08.

[22] University, C. "http://www.clean.cise.columbia.edu//process/spintheory.pdf", accessed 15/01/08.

[23] Roe, R.-J. *Methods of X-Ray and Neutron Scattering in Polymer Science (Topics in Polymer Science);* Oxford University Press: 2000.

[24] http://ssg.epfl.ch/images/SpinCoating.png, accessed 07/01/08.

[25] Kobashi, M.; Takeuchi, H.; Macromolecules **1998**, 31, 7273